

000 001 002 003 004 005 TUSOAI: AGENTIC OPTIMIZATION FOR SCIENTIFIC 006 METHODS 007 008 009

010 **Anonymous authors**
011 Paper under double-blind review
012
013
014
015
016
017
018
019
020
021
022
023
024
025
026
027
028
029
030
031

ABSTRACT

032 Scientific discovery is often slowed by the manual development of computational
033 tools needed to analyze complex experimental data. Building such tools is costly
034 and time-consuming because scientists must iteratively review literature, test mod-
035 eling and scientific assumptions against empirical data, and implement these in-
036 sights into efficient software. Large language models (LLMs) have demonstrated
037 strong capabilities in synthesizing literature, reasoning with empirical data, and
038 generating domain-specific code, offering new opportunities to accelerate com-
039 putational method development. Existing LLM-based systems either focus on
040 performing scientific analyses using existing computational methods or on de-
041 veloping computational methods or models for general machine learning without
042 effectively integrating the often unstructured knowledge specific to scientific do-
043 mains. Here, we introduce TusoAI, an agentic AI system that takes a scientific task
044 description with an evaluation function and autonomously develops and optimizes
045 computational methods for the application. TusoAI integrates domain knowledge
046 into a knowledge tree representation and performs iterative, domain-specific op-
047 timization and model diagnosis, improving performance over a pool of candidate
048 solutions. We conducted comprehensive benchmark evaluations demonstrating
049 that TusoAI outperforms state-of-the-art expert methods, MLE agents, and sci-
050 entific AI agents across diverse tasks. Applying TusoAI to two key open problems
051 in genetics improved existing computational methods and uncovered new biology
052 missed by previous methods.
053

1 INTRODUCTION

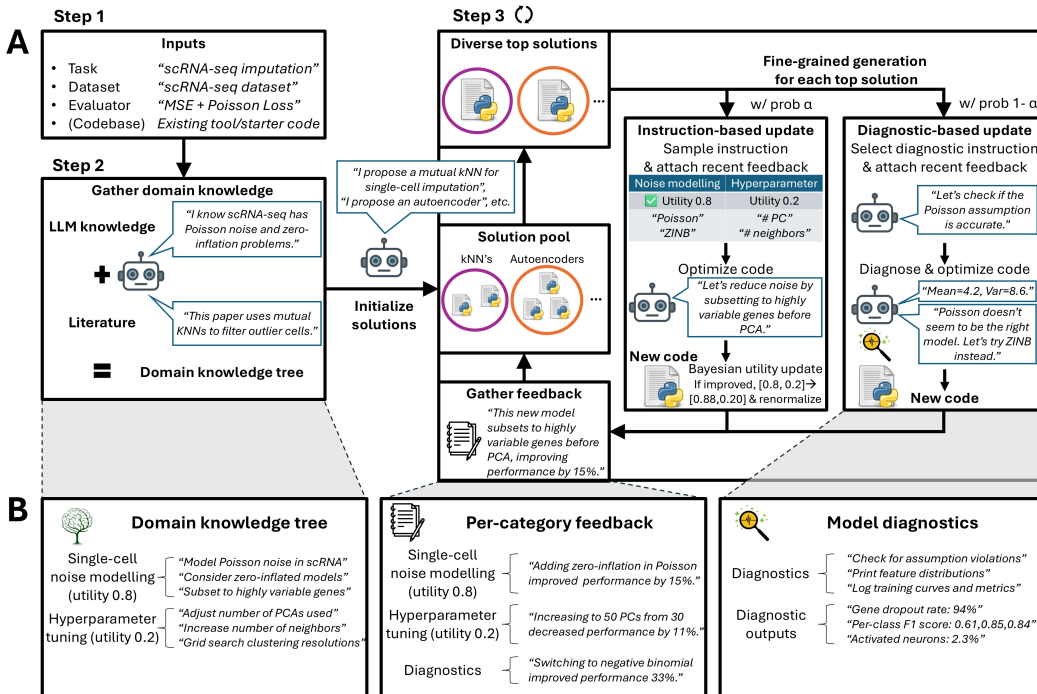
032 Scientific discoveries are often bottlenecked by the slow, manual development of computational
033 tools needed to analyze experimental data. For example, genetics studies have uncovered tens of
034 thousands of disease-associated variants, yet robust computational methods are critically needed to
035 harmonize multi-modal, multi-scale data and uncover the underlying mechanisms (Lappalainen &
036 MacArthur, 2021). Developing such tools is slow and costly because scientists must iteratively (i)
037 review extensive literature, (ii) test modeling and scientific assumptions against empirical data, and
038 (iii) implement these insights into efficient, scalable code. For instance, building robust computa-
039 tional methods to link enhancers with target genes from single-cell multiome data has taken multi-
040 ple expert groups many years (Dorans et al., 2025), hindered by challenges such as *cis*-regulatory
041 modeling, latent confounding, noisy data, and computational scalability. Large language models
042 (LLMs) have demonstrated strong capabilities in performing human-like analysis (Luo et al., 2025),
043 such as synthesizing relevant literature (Asai et al., 2024), reasoning about biological and modeling
044 assumptions using empirical data (Gao et al., 2024), and generating efficient, domain-specific code
045 (Rasheed et al., 2025). Integrating LLMs with scientific domain knowledge and iterative data exper-
046 imentation holds great promise to accelerate computational method development, thereby advancing
047 discoveries in science and medicine.
048

049 Existing work has produced general-purpose AI agents across scientific domains, including
050 biomedicine (Huang et al., 2025; Jin et al., 2025) and chemistry (M. Bran et al., 2024). These
051 systems primarily focus on performing scientific data analyses rather than developing new compu-
052 tational methods; the former involves assembling and executing pipelines of data formatting and
053 existing tools, whereas the latter requires creating new algorithms or models for specific pipeline
steps, involving substantial design, optimization, and validation. In parallel, several studies have

054 developed machine learning engineering (MLE) agents that can design new algorithms for general
 055 ML applications (Guo et al., 2024; Trirat et al., 2024; Jiang et al., 2025; Nam et al., 2025), but these
 056 approaches do not address domain-specific challenges inherent in scientific research. Developing
 057 *AI agents for scientific method development* that integrate structured domain knowledge and
 058 systematically explore data-specific assumptions has considerable potential to accelerate the creation
 059 of robust computational methods for science and medicine.

060 Here, we introduce TusoAI, an agentic AI system that takes a scientific task description with an
 061 evaluation function, and autonomously develops and optimizes computational methods for the appli-
 062 cation (Figure 1). TusoAI mimics a scientist’s cycle of method development, integrating structured
 063 domain knowledge with iterative, domain-specific optimization and model diagnosis, improving
 064 performance over a pool of candidate solutions. We demonstrate that TusoAI achieves superior per-
 065 formance across a range of algorithmic, statistical, machine learning, and deep learning applications
 066 in science. Our key contributions are:

- 068 1. We develop TusoAI, an AI agent specifically tailored for scientific method discovery by
 069 integrating structured domain knowledge.
- 070 2. We propose a novel framework, featuring (i) knowledge tree for structured representation
 071 of domain knowledge, (ii) hierarchical planning with Bayesian updates to balance solution
 072 quality and diversity, and (iii) fine-grained generation that integrates model optimization
 073 with diagnostic feedback.
- 074 3. We benchmark TusoAI on 6 single-cell analysis tasks and 5 scientific deep learning tasks,
 075 consistently outperforming baseline methods and frequently surpassing existing expert-
 076 designed algorithms.
- 077 4. Applying TusoAI to two key open problems in genetics improved existing computational
 078 methods and uncovered new biology missed by existing methods.



106 **Figure 1: Scientific method development with TusoAI. (A) Method overview. (B) Example do-**
 107 **main knowledge tree (categories and instructions per category), feedback, and diagnostics.**

108
109

1.1 RELATED WORK

110
111
112
113
114
115
116
117
118
119
120
121
122
123
124
125
126
127
128
129
130

LLM-based scientific AI agents. Several works have developed general-purpose AI agents capable of autonomously executing various scientific research tasks. Biomni (Huang et al., 2025) provides a unified agentic environment with tools and databases spanning 25 biomedical domains, integrating LLM reasoning with retrieval-augmented planning and code execution to compose complex workflows. Stella (Jin et al., 2025) employs a multi-agent architecture for autonomous biomedical data analysis, achieving self-evolution by dynamically updating its template library and tool collection. ChemCrow (M. Bran et al., 2024) is a chemistry-focused agent that integrates 18 expert-designed tools and follows the “Thought, Action, Action Input, Observation” format to iteratively reason toward answers. These methods emphasize end-to-end data analysis with established tools, whereas our work focuses on developing new computational methods for domain-specific tasks. Other works have leveraged LLMs to develop application-specific methods, such as single-cell perturbation prediction (Tang et al., 2025), diagnosis prediction (Tan et al., 2025), and mathematical discovery (Romera-Paredes et al., 2024). In contrast, TusoiAI targets computational method development across scientific tasks. InternAgent (Team et al., 2025) and its precursor Dolphin (Yuan et al., 2025) iteratively evolve and implement research ideas through an optimization process augmented with literature review. As a concurrent effort, Aygün et al. (2025) combine LLMs with tree search and existing model ensembles to improve scientific algorithms, addressing a similar problem but with a different approach from ours, which integrates a domain knowledge tree with fine-grained iterative optimization and Bayesian updates. As their code is not publicly available, direct comparison is not possible, but a key distinction of our work is to perform fine-grained optimizations with domain knowledge that do not require existing models and can operate on a small portion of a much larger method.

131
132
133
134
135
136
137
138
139
140
141
142
143

LLM-based general machine learning agents. Several recent works have developed AI agents for general machine learning engineering. AIDE (Jiang et al., 2025) frames ML engineering as a code optimization problem, combining an LLM with tree search to iteratively improve solutions. R&D Agent (Yang et al., 2025) similarly explores ML architectures in a dynamic feedback loop. DS-Agent (Guo et al., 2024) combines an LLM with case-based reasoning (CBR), retrieving potentially successful solutions from top-ranked Kaggle solutions, and refining them through iterative optimization. MLE-STAR (Nam et al., 2025) retrieves candidate models from the web to form an initial solution, then improve it by targeting specific ML components and ensembling. AutoML-Agent (Trirat et al., 2024) employs retrieval-augmented planning and multi-agent coordination to generate an optimal plan, but executes the plan once without iterative refinement. These methods are less suited to scientific method development, where domain knowledge is unstructured, existing ML models may be unavailable, and search spaces are continually evolving. We address these challenges through structured domain knowledge representation and a novel hierarchical planning procedure with Bayesian updates during iterative optimization.

144
145
146
147
148
149
150
151
152
153
154

Classical automatic machine learning (AutoML) frameworks. Classical (non-LLM) AutoML frameworks aim to construct high-performing ML models from scratch by searching over key components such as feature preprocessing, model architectures, hyperparameters, and pipeline composition. Notable examples include auto-sklearn (Feurer et al., 2015), H2O (LeDell et al., 2020), AutoGluon (Erickson et al., 2020), and TPOT (Olson & Moore, 2016). Within deep learning, neural architecture search (NAS) methods specialize in optimizing neural architectures, with examples such as DARTS (Liu et al., 2018) and AMBER (Zhang et al., 2021). While effective for standard ML tasks, these approaches are constrained by predefined search spaces and are less suited to scientific domains, where domain knowledge and optimization objectives are unstructured and continually evolving, making LLM-based agents a more natural fit as they can pair a principled optimization objective with heuristic search procedures.

155
156
157

2 PROBLEM FORMULATION

158
159
160
161

We consider the problem of automatic scientific algorithm optimization with LLMs. Given a general solution space $\mathcal{S}^{\text{full}}$ (e.g., all Python scripts) and an evaluator $h(\cdot) : \mathcal{S}^{\text{full}} \mapsto \mathbb{R}$, the objective is to find the optimal solution $s^* = \arg \max_{s \in \mathcal{S}^{\text{full}}} h(s)$. $h(\cdot)$ can be any evaluation metric, such as AUC, average of several metrics, or domain-specific measures (e.g., enrichment of inferred disease genes against an expert-curated set). We assume access to a task description \mathcal{T} (e.g., “single-cell RNA-seq

162 imputation”), a domain-specific knowledge base (e.g., scientific papers), and a general LLM that can
 163 be instantiated as agents. The agent can, for example, summarize domain priors from \mathcal{T} , retrieve
 164 information from the knowledge base, and refine a candidate solution s based on instructions. The
 165 goal is to iteratively implement and improve solutions to maximize $h(\cdot)$ within a time budget. We
 166 consider two settings: a *cold start*, where optimization begins from scratch, and a *warm start*, where
 167 an initial solution s_{init} (e.g., a state-of-the-art method) is given for further improvement.

3 METHODS

172 TusoAI takes as input a task description \mathcal{T} , a dataset \mathcal{D} , an evaluator $h(\cdot)$, and optionally an initial
 173 solution s_{init} . It outputs an optimized solution s^* (Algorithm 1, variables described in Appendix
 174 Table A). TusoAI operates on only a single function of an arbitrarily large codebase, allowing it
 175 to flexibly build upon scientific methods with extensive scaffolding. Developing computational
 176 methods for scientific domains poses several challenges. First, domain-specific knowledge is often
 177 unstructured, which we address using a knowledge tree that organizes information into categories
 178 and within-category instructions. Second, approaches and optimization strategies can vary widely,
 179 which we manage through hierarchical planning with Bayesian updates to promote diversity while
 180 ensuring solution quality. Third, understanding complex data patterns is challenging, which we
 181 mitigate with fine-grained generation that integrates model optimization with diagnostic feedback.

182 TusoAI consists of 3 steps. First, it gathers domain knowledge by summarizing key scientific
 183 papers, ensuring that optimization instructions reflect established best practices and recent advances
 184 rather than relying solely on LLM priors. Second, it builds a two-level knowledge tree of struc-
 185 tured instructions: (1) categories of optimization strategies and (2) specific instructions within each
 186 category, promoting both diversity and relevance. Categories and instructions are first drafted by
 187 the LLM and then refined through additional LLM queries in conjunction with paper summaries to
 188 ensure diversity and scientific rigor; we also predefine a diagnostic category $\mathcal{I}_{\text{diag}}$ to guide data log-
 189 ging and model diagnosis. Third, after initializing candidate solutions, it iteratively selects diverse
 190 top performers and improves them through either instruction-based or diagnostic-based optimiza-
 191 tion. Due to the knowledge tree structure, instruction categories can be sampled adaptively via a
 192 Bayesian strategy informed by past performance, while feedback comparing new and prior solu-
 193 tions helps discourage repetition. Examples of instructions generated are provided at Appendix C.

Algorithm 1 TusoAI

195 **Input:** Task \mathcal{T} ; dataset \mathcal{D} ; evaluator $h(\cdot)$; optional initial solution s_{init} .
 196 **Hyperparameters:** Time budget T_{budget} (default 8 hrs).
 197 1: **Gather domain knowledge:** $\mathcal{P} \leftarrow A_{\text{paper}}(\mathcal{T})$ ▷ Paper summaries
 198 2: **Build structured instructions:**
 199 $\mathcal{C}, \{\pi_c\}_{c \in \mathcal{C}} \leftarrow \text{DraftThenRefine}(A_{\text{cate}}, \mathcal{T}, \mathcal{P})$ ▷ Instruction categories with probabilities
 200 **For each** $c \in \mathcal{C}$:
 201 $\mathcal{I}_c \leftarrow \text{DraftThenRefine}(A_{\text{instr}}, \mathcal{T}, \mathcal{P}, c), \mathcal{F}_c \leftarrow \emptyset$ ▷ Per-category instructions and feedback
 202 $\mathcal{I}_{\text{diag}} \leftarrow \mathcal{I}_{\text{diag}}^{\text{predefined}}, \mathcal{F}_{\text{diag}} \leftarrow \emptyset$ ▷ Diagnostic instructions (predefined) and feedback
 203 3: **Initialize solutions:** $\mathcal{S} \leftarrow A_{\text{init}}(\mathcal{T}, \mathcal{P}, s_{\text{init}}); N_{\text{top}} \leftarrow |\mathcal{S}|$
 204 4: **While** wall-clock time $< T_{\text{budget}}$ **do**
 205 5: Select N_{top} diverse top solutions from \mathcal{S}
 206 6: **for each** top s **do**
 207 7: **if** $\text{Bernoulli}(\alpha)$ **do** ▷ Instruction-based optimization, defualt $\alpha = 0.8$
 208 8: Sample $c \sim \text{Cat}(\{\pi_c\}_{c \in \mathcal{C}})$; optimize $s' \leftarrow A_{\text{optim}}(s, \mathcal{I}_c, \mathcal{F}_c)$
 209 9: **if** $h(s') > h(s)$ **do** $\pi_c \leftarrow 1.1\pi_c$; renormalize $\{\pi_c\}_{c \in \mathcal{C}}$ ▷ Bayesian update utility
 210 10: $\mathcal{F}_c \leftarrow \mathcal{F}_c \cup \{A_{\text{feedback}}(s, s')\}$ ▷ Gather category-specific feedback
 211 11: **else** ▷ Diagnostic-based optimization
 212 12: $s' \leftarrow A_{\text{diag}}(s, \mathcal{D}, \mathcal{I}_{\text{diag}}, \mathcal{F}_{\text{diag}})$ ▷ Get model&data log info then optimize
 213 13: $\mathcal{F}_{\text{diag}} \leftarrow \mathcal{F}_{\text{diag}} \cup \{A_{\text{feedback}}(s, s')\}$ ▷ Gather diagnostic feedback
 214 14: $\mathcal{S} \leftarrow \mathcal{S} \cup \{s'\}$
 215 15: $N_{\text{sol}} \leftarrow \max(1, N_{\text{top}} - 1)$ every 2 rounds
 216 16: **return** $s^* \in \arg \max_{s \in \mathcal{S}} h(s)$

216 **Step 1: Gather domain knowledge.** TusoAI first retrieves up to 10 key papers from Semantic
 217 Scholar (Allen Institute for AI, 2025) relevant to \mathcal{T} , ranked by their citation count. For each paper,
 218 an agent A_{paper} creates a 15-point technical summary from the abstract and iteratively refines it
 219 using each paragraph of the paper’s Methods section (up to 1,200 words to focus solely on technical
 220 content without relying on costly deep research agents parsing the entire document). This produces
 221 $\mathcal{P} = \{\mathcal{P}_i\}$, where each \mathcal{P}_i is a refined 15-point summary of paper i ’s method.

222 **Step 2: Build structured instructions.** TusoAI uses a draft-then-refine strategy to construct optimi-
 223 zation categories, where an agent A_{cate} first drafts candidate categories from the task description
 224 \mathcal{T} , then refines them by iterating through each paper summary $\mathcal{P}_i \in \mathcal{P}$, adjusting existing categories
 225 or adding new ones as needed. Categories are task-specific and can be general (e.g., “regularization”,
 226 “model architectures”) or domain-specific (e.g., “single-cell noise modeling”, “genetic feature in-
 227 teractions”). Each category is assigned a probability π_c representing its utility in the optimization
 228 process; π_c is initialized by A_{cate} so that tasks earlier in the pipeline (e.g., “feature preprocessing”)
 229 receive higher weight than later ones (e.g., “hyperparameter tuning”). Similarly, TusoAI uses a
 230 draft-then-refine strategy to initialize instructions for each category, where an agent A_{instr} first drafts
 231 10 candidate instructions \mathcal{I}_c from the task description \mathcal{T} . These instruction lists are then refined by
 232 incorporating 10 additional instructions for each paper summary $\mathcal{P}_i \in \mathcal{P}$. For feedback, TusoAI ini-
 233 tializes an empty list $\mathcal{F}_c \leftarrow \emptyset$ for each category, which is updated with category-specific feedback
 234 during optimization. A special predefined diagnostic category $\mathcal{I}_{\text{diag}}$ provides instructions for logging
 235 diagnostic information useful for model updates, with its own feedback list $\mathcal{F}_{\text{diag}}$. See Appendix C,
 236 G for an example of constructed task information and Appendix U for prompt templates used to
 237 generate this information.

238 **Step 3.1: Initialize solutions.** The initialization agent A_{init} drafts 5 candidate solution descrip-
 239 tions from \mathcal{T} and iteratively refines them using each paper summary in \mathcal{P} , adding new descriptions
 240 or improving existing ones (e.g., “zero-inflated Poisson with kNN smoothing”). These are basic
 241 descriptions designed to start from scratch and explore to avoid simply re-implementing existing
 242 solutions. It then attempts to implement and debug each solution; those that successfully compile
 243 form the initial solution pool \mathcal{S} . Each implementation attempt is limited to 10 minutes with up to 4
 244 bug-fix attempts.

245 **Step 3.2: Iterative optimization.** Given the current solution set \mathcal{S} , TusoAI selects diverse top
 246 solutions by clustering them based on code-text similarity and, within each cluster, choosing the
 247 shortest solution whose performance is within 0.1% of the cluster’s best model; this helps discourage
 248 overfitting and randomness while maintaining diversity and concise code. For each cluster’s top
 249 solution s , TusoAI performs either instruction-based optimization (80% probability) or diagnostic-
 250 based optimization (20% probability). The resulting solution s' is added to the pool $\mathcal{S} \leftarrow \mathcal{S} \cup s'$.
 251 Each implementation attempt is limited to 10 minutes with up to 2 bug-fix attempts. This time
 252 regularization ensures the optimization period is not wasted on a few inefficient implementations,
 253 and encourages the final method to be scalable.

- 254 • **Instruction-based optimization.** The optimization agent A_{optim} selects an instruction by
 255 first sampling an instruction category $c \sim \text{Cat}(\{\pi_c\}_{c \in \mathcal{C}})$, then uniformly draw 3 candi-
 256 date instructions from \mathcal{I}_c , and finally choosing the most promising among them. It then
 257 optimizes s to produce s' using the selected instruction in conjunction with 5 most recent
 258 feedback entries from \mathcal{F}_c . If $h(s') > h(s)$, TusoAI performs a Bayesian-style update to the
 259 category utility by setting $\pi_c \leftarrow 1.1\pi_c$ and renormalizing $\{\pi_c\}_{c \in \mathcal{C}}$, representing the prior
 260 belief that this category currently contains useful instructions. Finally, the feedback agent
 261 A_{feedback} summarizes the change from s to s' and appends it to \mathcal{F}_c (e.g., “this optimization
 262 constructed a kNN on the top 50 PC’s rather than on all genes, improving performance by
 263 15%”).
- 264 • **Diagnostic-based optimization.** The optimization agent A_{optim} selects an instruction by
 265 first uniformly draw 3 candidate instructions from $\mathcal{I}_{\text{diag}}$ and then choosing the most promis-
 266 ing among them (e.g., “training curves”, “distribution checks”, “validation of assump-
 267 tions”). It then diagnoses and improves s to produce s' using the selected instruction in
 268 conjunction with 5 most recent feedback entries from \mathcal{F}_c : it runs s to collect diagnostic
 269 logs and then uses this information to produce an improved model s' . This represents a sci-
 270 entist diagnosing their method’s intermediate outputs to further improve upon it. Finally,
 271 the feedback agent A_{feedback} summarizes the change from s to s' and appends it to $\mathcal{F}_{\text{diag}}$.

270

4 EXPERIMENTS

271
 272 We evaluate TusoAI on 11 scientific applications spanning diverse domains with both ML and non-
 273 ML components, including 6 single-cell analysis tasks (Luecken et al., 2025) and 5 scientific deep
 274 learning tasks (Tu et al., 2022). The single-cell tasks include denoising (Denoise), cell-type la-
 275 bel projection (Label), batch integration (Batch), identification of spatially variable genes (SVG),
 276 decomposition of spot-level spatial data into specific cell types (Decomp), and dimensionality re-
 277 duction for visualization (Visual). The scientific deep learning tasks include omnidirectional vision
 278 (Spherical), prosthetics control (NinaPro), medical diagnostics (ECG), earth monitoring (Satellite),
 279 and genetic prediction (DeepSea). In each task, we run TusoAI for 8 hours (as per related work
 280 (Miller et al., 2025; Aygün et al., 2025)), optimizing performance on a validation dataset, and eval-
 281 uating final performance on separate testing datasets. Task descriptions used are concise (e.g., “single-
 282 cell batch integration”) and extracted from the original benchmarks. We define Avg. and Avg. Rank
 283 as the average performance across tasks for a method, and the average rank in each task, respec-
 284 tively. We additionally assess code diversity, defined as the text similarity between generated code
 285 (Appendix M) and mean time to optimize, defined as the average position of each optimization over
 286 the 8 hours, representing how quickly optimizations are achieved.

287 We conduct comprehensive ablation studies to assess the contribution of different components of
 288 TusoAI (Subsection 4.2), and two case studies demonstrating how TusoAI can reveal new biological
 289 insights in genetics (Section 5). Full details on experimental setup and evaluation metrics used are
 290 in Appendix D, E for single-cell and deep learning tasks, respectively.

291 **Baseline methods.** We compare TusoAI against the state-of-the-art MLE agent AIDE (Jiang et al.,
 292 2025), scientific agents Biomni (Huang et al., 2025) and ChatGPT-Agent (OpenAI, 2025), and top-
 293 performing, published application-specific methods. Biomni (LLM backbone Claude-4-Sonnet) and
 294 ChatGPT-agent (LLM backbone GPT-5) are used to iteratively build models on data for single-
 295 cell tasks; for deep learning tasks, where Biomni and ChatGPT-agent were unable to operate, we
 296 substitute the best of ten models constructed by Claude-4-Sonnet and GPT-5. GPT-4o-mini and
 297 GPT-5 are accessed through the OpenAI API, and all others with OpenRouter. For application-
 298 specific baselines, we use the “top-performing expert” method for single-cell tasks (Luecken et al.,
 299 2025), and all baseline methods, including expert models and NAS methods, for the scientific deep
 300 learning tasks (Tu et al., 2022). This set of baselines is consistent with related work in scientific
 301 optimization (Aygün et al., 2025) and a recent benchmark that identified AIDE and Biomni as top-
 302 performers (Miller et al., 2025). We note that most MLE agentic methods cannot apply to scientific
 303 tasks outside the standard ML setup. For full details on baseline implementation and setup, see
 304 Appendix F.

305

4.1 PERFORMANCE ACROSS BENCHMARK EXPERIMENTS

306 Results for the 6 single-cell tasks and 5 scientific deep learning tasks are reported in Tables 1 and 2.
 307 We reached 2 main conclusions. First, TusoAI consistently outperformed baseline methods across
 308 benchmarks when generating code from scratch (average rank of 1.2 for single-cell tasks and 2.8 for
 309 scientific deep learning tasks, vs. 3.0 and 4.0 for the second best, resp.). Second, the methods con-
 310 structed by TusoAI are novel rather than simple re-implementations of existing approaches or calls
 311 to standard packages. Examples include: (i) in single-cell denoise, TusoAI designed a non-negative
 312 matrix factorization (NMF) approach that models dropout rates, Poisson noise, and performs itera-
 313 tive refinement, distinct from the only other NMF-based approach in the OpenProblems benchmark,
 314 ALRA (Linderman et al., 2022); (ii) in SVG, TusoAI adapted known techniques such as modeling
 315 expression as a function of spatial coordinates and neighborhood summaries to create a custom,
 316 high-performing method; (iii) in Satellite, TusoAI combined preprocessing, training procedures,
 317 loss functions, and ensembling techniques to build the top-performing model; and (iv) in Spherical,
 318 TusoAI fine-tuned layers of ResNet-50 and augmented the data with random flips and rotations.
 319 See Appendix H for full justification of why these new methods are novel. Third, all methods con-
 320 structed by TusoAI are computationally efficient (<3 minutes for single-cell tasks and <8 minutes
 321 for deep learning tasks, Appendix I), owing to the runtime constraints imposed during optimiza-
 322 tion.

323 We conducted 2 secondary analyses. First, we assessed the diversity of code produced by TusoAI
 324 and AIDE over 8 hours of optimization, quantifying code diversity using cosine similarity of text
 325 embeddings between each candidate and its 10 previous and 10 subsequent iterations (Figure 2A).

	Denoise	Label	Batch	SVG	Decomp	Visual	Avg	Avg rank
Expert	0.28	0.85	0.71	0.66	0.49	0.44	<u>0.57</u>	3.7
AIDE*	<u>0.30</u>	0.87	0.71	<u>0.73</u>	0.06	0.44	0.52	<u>3.0</u>
Biomni*	0.16	0.89	0.82	0.16	0.53	0.35	0.49	3.7
ChatGPT-Agent*	0.03	0.81	0.83	0.60	0.74	0.38	<u>0.57</u>	3.5
TusoAI*	0.35	0.89	0.83	0.80	<u>0.64</u>	0.44	0.66	1.2

Table 1: **Single-cell benchmarks.** We report performance across 6 single-cell tasks. “*” denotes agentic methods. Best in **bold**, second-best underlined. 95% CIs across 3 random seeds all under 0.01 and thus not shown.

	Spherical	NinaPro	ECG	Satellite	DeepSEA	Avg	Avg rank
WRN default	0.14 ± 0.01	0.93 ± 0.00	0.57 ± 0.00	0.85 ± 0.00	0.60 ± 0.00	0.62	6.9
DenseNAS random	0.29 ± 0.02	0.92 ± 0.01	0.58 ± 0.00	0.86 ± 0.00	0.60 ± 0.00	<u>0.65</u>	5.4
DenseNAS original	0.27 ± 0.01	0.90 ± 0.01	0.60 ± 0.00	0.86 ± 0.01	0.60 ± 0.00	<u>0.65</u>	5.8
Perceiver IO	0.17 ± 0.00	0.78 ± 0.02	0.34 ± 0.00	0.84 ± 0.00	0.62 ± 0.00	0.55	9.6
XGBoost	0.03 ± 0.00	0.78 ± 0.01	0.44 ± 0.00	0.64 ± 0.00	0.50 ± 0.00	0.48	11.6
WRN ASHA	0.25 ± 0.00	0.93 ± 0.01	0.57 ± 0.00	0.84 ± 0.01	0.59 ± 0.00	0.63	7.1
DARTS	0.52 ± 0.03	0.82 ± 0.01	0.66 ± 0.00	0.87 ± 0.00	0.68 ± 0.00	0.71	<u>4.0</u>
AMBER	N/A	N/A	<u>0.67</u> ± 0.00	0.87 ± 0.00	0.68 ± 0.00	N/A	N/A
Expert	0.33 ± 0.01	0.91 ± 0.01	0.72 ± 0.00	0.80 ± 0.00	0.70 ± 0.00	0.69	4.6
AIDE*	0.16 ± 0.01	0.86 ± 0.00	0.52 ± 0.01	0.83 ± 0.01	0.57 ± 0.00	0.59	9.8
GPT-5*	0.36 ± 0.00	0.89 ± 0.00	0.58 ± 0.03	0.86 ± 0.01	0.66 ± 0.00	0.67	5.8
Claude-4-Sonnet*	0.40 ± 0.00	0.90 ± 0.00	0.50 ± 0.01	0.88 ± 0.00	0.73 ± 0.00	0.68	4.6
TusoAI*	0.42 ± 0.01	0.90 ± 0.00	0.61 ± 0.00	0.89 ± 0.01	0.70 ± 0.00	0.70	2.8

Table 2: **Scientific deep learning benchmarks.** We report performance across 5 scientific deep learning tasks. “*” denotes agentic methods. Performance of non-agentic methods extracted from NASBENCH-360 and transformed to be between 0 and 1 and higher is better. Best in **bold**, second-best underlined. 95% CIs provided across 3 random seeds.

We note that constructing diverse code to escape local optima is often an important consideration in agentic code optimization (Romera-Paredes et al., 2024; Nam et al., 2025; Aygün et al., 2025). TusoAI achieved substantially higher diversity than AIDE throughout the optimization process. For example, in the batch integration benchmark, AIDE repeatedly proposed small variations of UMAP-based dimensionality reduction, whereas TusoAI explored a wide variety of dimensionality reduction, transformation, and scaling techniques. This higher diversity is perhaps due to TusoAI’s instruction sampling, feedback, and diagnosis procedures, which encourage diverse solutions. We validate the importance of code diversity in generating strong optimizations (Appendix M). In contrast, AIDE promotes incremental changes at each optimization step to facilitate traceability, which may bias the search toward local tuning rather than full exploration. Second, we characterized the optimization trajectory of TusoAI on the single-cell denoising task (Figure 2B). We identified 5 key developments that led to strong performance: (1) introducing NMF, (2) modeling dropout, (3) modeling Poisson noise, (4) adding iterative refinement, and (5) incorporating a sparsity-balancing step. Notably, during optimization, TusoAI generated many methods that reduced performance before converging on high-performing solutions. Together with the feedback mechanism, this broad exploration allowed TusoAI to efficiently search the solution space and identify top-performing methods. See Appendix J, K for the optimization trajectories in other tasks.

4.2 ABLATION STUDIES

We conducted extensive ablation studies to evaluate the impact of each novel component of TusoAI by removing one at a time, including: (i) removing the categorical structure and placing all instructions and feedback into a single category (No categories); (ii) disabling the Bayesian sampling strategy across categories (No Bayesian); (iii) disabling the model diagnosis capability (No diagnosis); and (iv) discarding domain knowledge altogether, such that each iteration simply applies a generic instruction (e.g., “Optimize this model”; No knowledge). Removing these components each negatively affected overall performance (Table 3). We attribute this to reduced code diversity

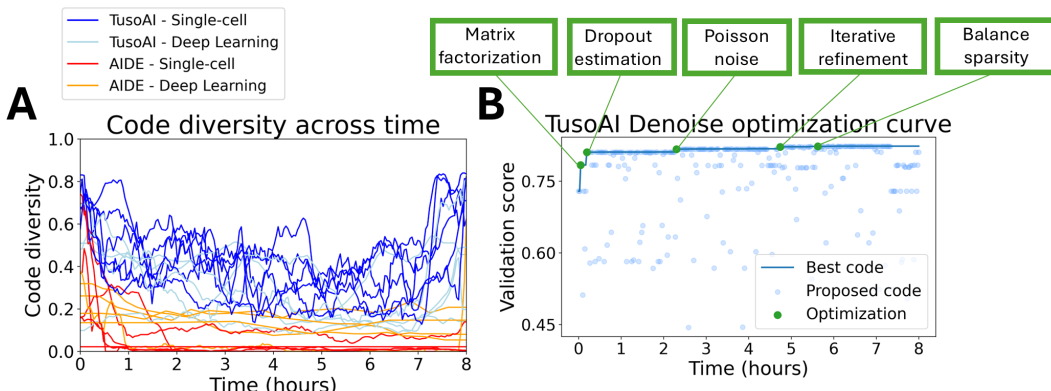


Figure 2: **Behavior of code generated by TusoAI.** (A) Code diversity of TusoAI and AIDE over optimization time, as measured by $1 - \cosine$ similarity. Each line corresponds to a dataset. (B) Performance of the proposed optimization and the best code over optimization time for a representative task “Denoise”. Key optimization changes with their occurrence times are annotated.

(mean diversity 0.48 vs. 0.44/0.39/0.38/0.33 for ablated versions, resp.) and computational efficiency (mean time to optimize 2.3 hours vs. 2.4/3.0/2.6/2.4 for ablated versions, resp.). Removing domain knowledge had the strongest impact on performance and diversity, while removing Bayesian updates (thus sampling categories uniformly) most reduced TusoAI’s computational efficiency. See Appendix L, N, O for TusoAI’s general stability across replicates, further ablation details and ablations varying literature information used.

We next assessed the impact of LLM backbones used by TusoAI, testing across 5 different LLMs: low-latency models GPT-4o-mini (default) and Claude-3.5-Haiku; state-of-the-art reasoning models GPT-5 and Claude-4-Sonnet; and open-source GPT-oss-120b. Results are shown in Table 3. Apart from GPT-oss-120b, TusoAI achieved relatively consistent performance across all LLMs for most tasks, demonstrating robustness. Interestingly, LLMs such as GPT-5 and Claude-4-Sonnet did not consistently outperform their lower-latency counterparts, GPT-4o-mini and Claude-3.5-Haiku. This may be because, while reasoning models can construct highly complex code, their tendency to over-build (e.g., each of GPT-5’s methods are 300+ lines of code) makes subsequent iterations difficult to refine; in contrast, low-latency but capable models like GPT-4o-mini and Claude-3.5-Haiku, when paired with an appropriate system design, performed just as well at a fraction of the cost (e.g., optimizing denoising for 8 hours costs 0.24\$ with GPT-4o-mini and 22.3\$ with GPT-5). See Appendix P, Q for further LLM analysis and cost details, respectively.

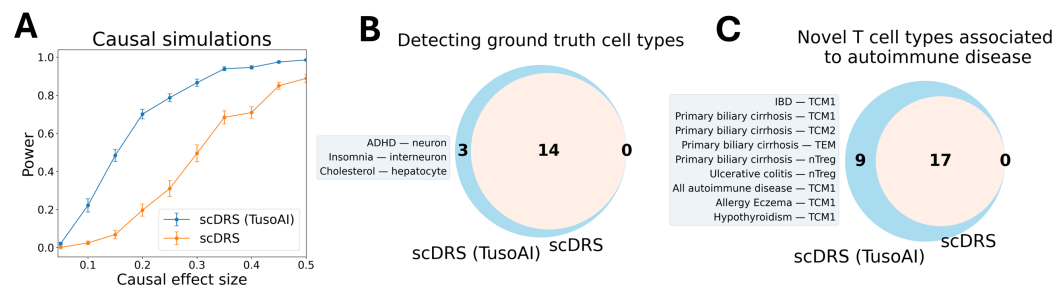
	Denoise	SVG	Decomposition	ECG	Satellite	Avg	Avg rank
TusoAI (default)	<u>0.35</u>	0.80	0.64	0.61	0.89	0.66	2.0
No categories	0.09	0.72	0.56	<u>0.63</u>	0.86	0.57	3.2
No Bayesian	0.36	0.77	0.22	0.57	0.84	0.55	3.4
No diagnosis	0.26	0.77	0.68	0.63	0.86	0.64	2.0
No knowledge	0.17	0.51	0.07	0.68	0.85	0.46	3.8
GPT-4o-mini (default)	0.35	0.80	0.64	0.61	0.89	0.66	2.2
GPT-5	0.31	0.80	0.82	0.67	0.87	0.69	2.2
Claude 3.5 Haiku	0.41	0.78	0.70	<u>0.63</u>	0.89	0.68	1.8
Claude 4 Sonnet	0.32	0.78	0.53	0.59	0.84	0.61	4.2
GPT-oss-120b	0.39	0.74	0.13	0.61	0.85	0.54	3.8

Table 3: **Ablation studies (top) and varying LLM backbone (bottom).** Best in **bold**, second-best underlined.

432 5 CASE STUDIES IN GENETICS

434 We applied TusoAI to address 2 key challenges in genetics: detecting disease-critical cell populations
 435 and linking genetic variants to their target genes; these are central to understanding disease
 436 etiology but limited by current computational models. We initialized TusoAI with state-of-the-art
 437 methods (scDRS (Zhang et al., 2022b) and pgBoost (Dorans et al., 2025), resp.) and evaluated its
 438 ability to improve these approaches and generate new biological insights. We consider the same
 439 quantitative evaluation procedure and level of validation for new discoveries as in the original pa-
 440 pers. We note these codebases are too large to easily use with existing agentic approaches that
 441 require editing the entire Python script. See full details of how we applied TusoAI to each task in
 442 Appendix R, S for scDRS and pgBoost, respectively. An additional case study of how TusoAI may
 443 optimize an existing deep learning model outside of biology is in Appendix T.

444 **Detecting disease-critical cell populations.** scDRS (Zhang et al., 2022b) is a state-of-the-art
 445 method that integrates genome-wide association studies (GWAS) with single-cell RNA-seq (scRNA-
 446 seq) to identify disease-associated cell populations, but its power is limited by the high noise of
 447 scRNA-seq data. Here, we apply TusoAI in conjunction with scDRS and task it with optimizing
 448 scDRS’s association scoring function. Results are reported in Figure 3. We reached 3 main con-
 449 clusions. First, the TusoAI-optimized version substantially outperformed the original scDRS in both
 450 simulations and real-data benchmarks: it achieved over 40% higher power in causal simulations
 451 (Figure 3A) while retaining calibration in null settings (Appendix R), and identified 21% more true
 452 cell type–disease associations (17 vs. 14) without false associations in a real-data benchmark (Li
 453 et al., 2025). Second, the TusoAI-optimized scoring function is concise and interpretable. It com-
 454 putes association scores in *log–log* rather than *log* space, likely because this transformation better
 455 captures polygenic disease signals across many genes, avoiding domination by a few highly ex-
 456 pressed genes. This improvement reflects TusoAI’s ability to efficiently explore variations built on
 457 the original method: it tested 167 different variations in 24 hours and at a cost of \$0.37, whereas
 458 the original authors evaluated fewer than 10 versions over 3 months. Third, applying the TusoAI-
 459 optimized scDRS to a T cell dataset (Cano-Gomez et al., 2020) revealed 26 disease-associated T cell
 460 subpopulations (at $FDR < 0.05$, as per original paper) vs. 17 by the original method, including regu-
 461 latory T cells, central memory T cells, and effector memory T cells associated with primary biliary
 462 cirrhosis, consistent with the roles of these T cell populations in autoimmunity (Dominguez-Villar
 463 & Hafler, 2018; Seo et al., 2025).



474 **Figure 3: Optimizing scDRS for detecting cell-disease associations.** (A) Assessing power in
 475 causal simulations. 95% CI’s are calculated across 30 replicates at each perturbation effect size. (B)
 476 Venn diagram of discovered ground-truth trait-cell type pairs at $FDR < 0.05$ for scDRS and scDRS
 477 (TusoAI). New trait-cell type pairs are indicated on the left. (C) Venn diagram of discovered trait-
 478 T cell subtype pairs at $FDR < 0.05$ for scDRS and scDRS (TusoAI). New trait-cell type pairs are
 479 indicated on the left.

480 **Linking genetic variants to genes using single-cell multiome.** pgBoost (Dorans et al., 2025) is a
 481 state-of-the-art method for linking genetic variants to target genes using single-cell multiome data;
 482 it integrates variant–gene distance with multiple linking strategies, but the task remains challenging
 483 due to the complexity of genetic regulation (Gazal et al., 2022). Here, we apply TusoAI in con-
 484 junction with pgBoost, providing additional positional information for variants and genes, and task
 485 it with optimizing distance-based features. Results are reported in Figure 4. We reached 3 main

conclusions. First, the TusoAI-optimized model significantly outperformed the original pgBoost, achieving 13.8% higher enrichment of gold-standard links from fine-mapped eQTLs and 7.2% from activity-by-contact (ABC) links, with particularly large gains across longer variant–gene distances where links are harder to identify (Figure 4A,B). Second, the distance-based features generated by TusoAI are concise and interpretable: 3 are transformed versions of existing features (inverse, squared, and normalized terms), 2 are interactions of gene annotations with distance terms, and the sixth indicates whether the SNP is $<50\text{kb}$ from the gene’s transcription start site, consistent with literature suggesting the typical enhancer–promoter range of around 70kb (Bower et al., 2025). TusoAI discovered these features by testing 511 combinations of 153 novel distance features within 24 hours at a cost of \$0.41, whereas the original authors evaluated 5 features over 1.5 months. Third, applying the TusoAI-optimized pgBoost to fine-mapped SNPs for 94 diseases/traits identified 7 new variant–gene links missed by previous methods ($> 95\%$ linking percentile vs. $< 95\%$ all others, as per original paper). For example, a fine-mapped variant rs138917529 for glucose and HbA1c was linked to *GCK*, consistent with the roles of Glucokinase in regulating glucose levels related to both glucose metabolism (Froguel et al., 1993) and HbA1c variation (Chakera et al., 2015).

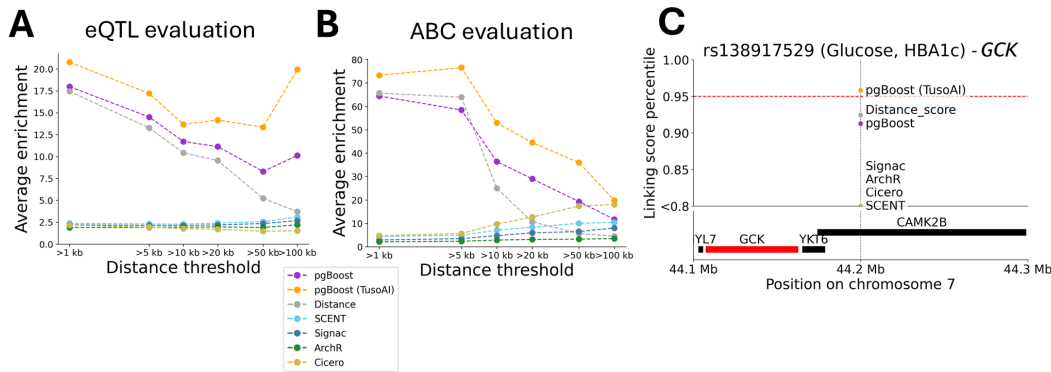


Figure 4: **Optimizing pgBoost for SNP-gene link discovery.** (A) Area under the enrichment-recall curve (AUERC, as defined in pgBoost) across distance thresholds for ground truth eQTL variant-gene links. (B) AUERC across distance thresholds for ground truth ABC variant-gene links. (C) Locus plot of rs138917529 and surrounding genes. Red dashed line indicates linking score percentile cutoff for SNP-gene linking. *GCK* is shaded red, as the gene linked to the focal SNP.

6 DISCUSSION

We have presented TusoAI, an agentic system for scientific method optimization. By mimicking a scientist’s cycle of method development, TusoAI achieves superior performance on single cell and scientific deep learning benchmarks, and is further able to discover significant optimizations to state of the art methods in genetics which revealed new biology missed by existing methods. We believe TusoAI represents a promising step towards automated scientific method development and optimization, thus accelerating scientific discovery.

We acknowledge several limitations and areas for future work. TusoAI requires a separate validation experiment to base optimization on to prevent overfitting. This experiment should also be quick to run while representing final performance. When optimizing an existing method, TusoAI performs strongest when most of the method is in a single function, and may not perform well if the method is scattered throughout a large codebase. TusoAI does not consider making new evaluation procedures, but rather relies on existing ones and will be vulnerable to the same weaknesses those may have. Several algorithm components are heuristic and may benefit from theoretic justification. We generally focus on biological applications given their complexity and relevance, but achieve reliable performance in diverse scientific domains. Future work may include processing multiple functions in parallel by treating them as separate subtasks, or searching over not just the code-space for methods, but also the data-space for additional useful data to include in a method, as is common in scientific domains.

540 REFERENCES
541

542 Hananeh Aliee and Fabian J Theis. Autogenes: Automatic gene selection using multi-objective
543 optimization for rna-seq deconvolution. *Cell Systems*, 12(7):706–715, 2021.

544 Allen Institute for AI. Semantic scholar. <https://www.semanticscholar.org>, 2025. Ac-
545 cessed: 2025-09-16.

546 Alma Andersson and Joakim Lundeberg. sepal: Identifying transcript profiles with spatial patterns
547 by diffusion-based modeling. *Bioinformatics*, 37(17):2644–2650, 2021.

548 Akari Asai, Jacqueline He, Rulin Shao, Weijia Shi, Amanpreet Singh, Joseph Chee Chang, Kyle
549 Lo, Luca Soldaini, Sergey Feldman, Mike D’arcy, et al. Openscholar: Synthesizing scientific
550 literature with retrieval-augmented lms. *arXiv preprint arXiv:2411.14199*, 2024.

551 Eser Aygün, Anastasiya Belyaeva, Gheorghe Comanici, Marc Coram, Hao Cui, Jake Garrison, Re-
552 nee Johnston Anton Kast, Cory Y McLean, Peter Norgaard, Zahra Shamsi, et al. An ai system to
553 help scientists write expert-level empirical software. *arXiv preprint arXiv:2509.06503*, 2025.

554 Nuha BinTayyash, Sokratia Georgaka, ST John, Sumon Ahmed, Alexis Boukouvalas, James Hens-
555 man, and Magnus Rattray. Non-parametric modelling of temporal and spatial counts data from
556 rna-seq experiments. *Bioinformatics*, 37(21):3788–3795, 2021.

557 G. Bower, E. W. Hollingsworth, S. H. Jacinto, et al. Range extender mediates long-distance enhancer
558 activity. *Nature*, 643:830–838, 2025. doi: 10.1038/s41586-025-09221-6.

559 Guoxin Cai, Yichang Chen, Shuqing Chen, Xun Gu, and Zhan Zhou. Spanve: A statistical method
560 for detecting downstream-friendly spatially variable genes in large-scale spatial transcriptomic
561 data. *bioRxiv*, pp. 2023–02, 2023.

562 Enrique Cano-Gamez, Blagoje Soskic, Theodoros I. Roumeliotis, et al. Single-cell transcrip-
563 toomics identifies an effectorness gradient shaping the response of cd4+ t cells to cytokines. *Nature
564 Communications*, 11(1):1801, 2020. doi: 10.1038/s41467-020-15543-y. URL <https://doi.org/10.1038/s41467-020-15543-y>.

565 Ali J. Chakera, Anna M. Steele, Anna L. Gloyn, Maggie H. Shepherd, Beverley Shields, Sian Ellard,
566 and Andrew T. Hattersley. Recognition and management of individuals with hyperglycemia be-
567 cause of a heterozygous glucokinase mutation. *Diabetes Care*, 38(7):1383–1392, 06 2015. ISSN
568 0149-5992. doi: 10.2337/dc14-2769. URL <https://doi.org/10.2337/dc14-2769>.

569 Yuzhou Chang, Jixin Liu, Yi Jiang, Anjun Ma, Yao Yu Yeo, Qi Guo, Megan McNutt, Jordan E Krull,
570 Scott J Rodig, Dan H Barouch, et al. Graph fourier transform for spatial omics representation and
571 analyses of complex organs. *Nature Communications*, 15(1):7467, 2024.

572 Taco S Cohen, Mario Geiger, Jonas Köhler, and Max Welling. Spherical cnns. *arXiv preprint
573 arXiv:1801.10130*, 2018.

574 Angus Dempster, François Petitjean, and Geoffrey I Webb. Rocket: exceptionally fast and accu-
575 rate time series classification using random convolutional kernels. *Data Mining and Knowledge
576 Discovery*, 34(5):1454–1495, 2020.

577 Margarita Dominguez-Villar and David A. Hafler. Regulatory t cells in autoimmune disease.
578 *Nature Immunology*, 19:665–673, 2018. doi: 10.1038/s41590-018-0120-4. URL <https://doi.org/10.1038/s41590-018-0120-4>.

579 Elizabeth Dorans, Karthik Jagadeesh, Kushal Dey, and Alkes L Price. Linking regulatory variants to
580 target genes by integrating single-cell multiome methods and genomic distance. *Nature Genetics*,
581 pp. 1–10, 2025.

582 Nick Erickson, Jonas Mueller, Alexander Shirkov, Hang Zhang, Pedro Larroy, Mu Li, and Alexan-
583 der Smola. Autogluon-tabular: Robust and accurate automl for structured data. *arXiv preprint
584 arXiv:2003.06505*, 2020.

594 Zhangyin Feng, Daya Guo, Duyu Tang, Nan Duan, Xiaocheng Feng, Ming Gong, Linjun Shou, Bing
 595 Qin, Ting Liu, Dixin Jiang, and Ming Zhou. Codebert: A pre-trained model for programming and
 596 natural languages. *CoRR*, abs/2002.08155, 2020. URL <https://arxiv.org/abs/2002.08155>.

598 Matthias Feurer, Aaron Klein, Katharina Eggensperger, Jost Springenberg, Manuel Blum, and Frank
 599 Hutter. Efficient and robust automated machine learning. *Advances in neural information pro-*
 600 *cessing systems*, 28, 2015.

602 Philippe Froguel, Habib Zouali, Nathalie Vionnet, Gilberto Velho, Martine Vaxillaire, Fang Sun,
 603 Suzanne Lesage, Markus Stoffel, Jun Takeda, Philippe Passa, M. Alan Permutt, Jacques S. Beck-
 604 mann, Graeme I. Bell, and Daniel Cohen. Familial hyperglycemia due to mutations in glucokinase
 605 – definition of a subtype of diabetes mellitus. *New England Journal of Medicine*, 328(10):697–
 606 702, 1993. doi: 10.1056/NEJM199303113281005. URL <https://www.nejm.org/doi/full/10.1056/NEJM199303113281005>.

608 Shanghua Gao, Ada Fang, Yepeng Huang, Valentina Giunchiglia, Ayush Nouri, Jonathan Richard
 609 Schwarz, Yasha Ektelai, Jovana Kondic, and Marinka Zitnik. Empowering biomedical discovery
 610 with ai agents. *Cell*, 187(22):6125–6151, 2024.

611 Steven Gazal, Omer Weissbrod, Farhad Hormozdiari, Kushal K. Dey, Joseph Nasser, Kumar A.
 612 Jagadeesh, Daniel J. Weiner, Huwenbo Shi, Charles P. Fulco, Luke J. O'Connor, Bogdan
 613 Pasaniuc, Jesse M. Engreitz, and Alkes L. Price. Combining snp-to-gene linking strate-
 614 gies to identify disease genes and assess disease omnigenicity. *Nature Genetics*, 54(6):827–
 615 836, June 2022. doi: 10.1038/s41588-022-01087-y. URL <https://doi.org/10.1038/s41588-022-01087-y>.

617 Siyuan Guo, Cheng Deng, Ying Wen, Hechang Chen, Yi Chang, and Jun Wang. Ds-agent: Au-
 618 tomated data science by empowering large language models with case-based reasoning. *arXiv*
 619 *preprint arXiv:2402.17453*, 2024.

621 Minsheng Hao, Kui Hua, and Xuegong Zhang. Somde: a scalable method for identifying spatially
 622 variable genes with self-organizing map. *Bioinformatics*, 37(23):4392–4398, 2021.

623 Shenda Hong, Yanbo Xu, Alind Khare, Satria Priambada, Kevin Maher, Alaa Aljiffry, Jimeng Sun,
 624 and Alexey Tumanov. Holmes: health online model ensemble serving for deep learning models
 625 in intensive care units. In *Proceedings of the 26th ACM SIGKDD International Conference on*
 626 *Knowledge Discovery & Data Mining*, pp. 1614–1624, 2020.

627 Jian Hu, Xiangjie Li, Kyle Coleman, Amelia Schroeder, Nan Ma, David J Irwin, Edward B Lee,
 628 Russell T Shinohara, and Mingyao Li. Spagn: Integrating gene expression, spatial location and
 629 histology to identify spatial domains and spatially variable genes by graph convolutional network.
 630 *Nature methods*, 18(11):1342–1351, 2021.

632 Kexin Huang, Serena Zhang, Hanchen Wang, Yuanhao Qu, Yingzhou Lu, Yusuf Roohani, Ryan Li,
 633 Lin Qiu, Gavin Li, Junze Zhang, et al. Biomni: A general-purpose biomedical ai agent. *biorxiv*,
 634 pp. 2025–05, 2025.

635 Jaemin Jeon, Youjeong Suk, Sang Cheol Kim, Hye-Yeong Jo, Kwangsoo Kim, and Inuk Jung.
 636 Denoiseit: denoising gene expression data using rank based isolation trees. *BMC bioinformatics*,
 637 25(1):271, 2024.

638 Zhengyao Jiang, Dominik Schmidt, Dhruv Srikanth, Dixin Xu, Ian Kaplan, Deniss Jacenko, and
 639 Yuxiang Wu. Aide: Ai-driven exploration in the space of code. *arXiv preprint arXiv:2502.13138*,
 640 2025.

642 Ruofan Jin, Zaixi Zhang, Mengdi Wang, and Le Cong. Stella: Self-evolving llm agent for biomedical
 643 research. *arXiv preprint arXiv:2507.02004*, 2025.

644 David Josephs, Carson Drake, Andy Heroy, and John Santerre. semg gesture recognition with a
 645 simple model of attention. In *Machine Learning for Health*, pp. 126–138. PMLR, 2020.

647 Ilia Kats, Roser Vento-Tormo, and Oliver Stegle. Spatialde2: fast and localized variance component
 648 analysis of spatial transcriptomics. *Biorxiv*, pp. 2021–10, 2021.

648 Tuuli Lappalainen and Daniel G MacArthur. From variant to function in human disease genetics.
 649 *Science*, 373(6562):1464–1468, 2021.
 650

651 Erin LeDell, Sebastien Poirier, et al. H2o automl: Scalable automatic machine learning. In *Pro-
 652 ceedings of the AutoML Workshop at ICML*, volume 2020, pp. 24, 2020.

653 Ang Li, Tian Lin, Alicia Walker, Xiao Tan, Ruolan Zhao, Shuyang Yao, Patrick F. Sullivan, Jens
 654 Hjerling-Leffler, Naomi R. Wray, and Jian Zeng. Benchmarking methods integrating gwas and
 655 single-cell transcriptomic data for mapping trait-cell type associations. *medRxiv*, 2025. doi:
 656 10.1101/2025.05.24.25328275. URL <https://www.medrxiv.org/content/early/2025/06/05/2025.05.24.25328275>.
 657

658 Qiwei Li, Minzhe Zhang, Yang Xie, and Guanghua Xiao. Bayesian modeling of spatial molecular
 659 profiling data via gaussian process. *Bioinformatics*, 37(22):4129–4136, 2021.
 660

661 George C. Linderman, Jiajun Zhao, Maria Roulis, et al. Zero-preserving imputation of single-cell
 662 rna-seq data. *Nature Communications*, 13:192, 2022. doi: 10.1038/s41467-021-27729-z. URL
 663 <https://doi.org/10.1038/s41467-021-27729-z>.
 664

665 Hanxiao Liu, Karen Simonyan, and Yiming Yang. Darts: Differentiable architecture search. *arXiv
 666 preprint arXiv:1806.09055*, 2018.
 667

668 M. D. Luecken, S. Gigante, D. B. Burkhardt, et al. Defining and benchmarking open prob-
 669 lems in single-cell analysis. *Nature Biotechnology*, 43:1035–1040, 2025. doi: 10.1038/
 670 s41587-025-02694-w. URL <https://doi.org/10.1038/s41587-025-02694-w>.
 671

672 Xiaoliang Luo, Akilles Rechardt, Guangzhi Sun, Kevin K Nejad, Felipe Yáñez, Bati Yilmaz,
 673 Kangjoo Lee, Alexandra O Cohen, Valentina Borghesani, Anton Pashkov, et al. Large language
 674 models surpass human experts in predicting neuroscience results. *Nature human behaviour*, 9(2):
 305–315, 2025.
 675

676 Andres M. Bran, Sam Cox, Oliver Schilter, Carlo Baldassari, Andrew D White, and Philippe
 677 Schwaller. Augmenting large language models with chemistry tools. *Nature Machine Intelli-
 678 gence*, 6(5):525–535, 2024.
 679

680 Henry E. Miller, Matthew Greenig, Benjamin Tenmann, and Bo Wang. Bioml-bench: Evalu-
 681 ation of ai agents for end-to-end biomedical ml. *bioRxiv*, 2025. doi: 10.1101/2025.09.01.
 682 673319. URL <https://www.biorxiv.org/content/early/2025/09/07/2025.09.01.673319>.
 683

684 J. M. Mudge, S. Carbonell-Sala, M. Diekhans, et al. Gencode 2025: reference gene annotation
 685 for human and mouse. *Nucleic Acids Research*, 53(D1):D966–D975, 2025. doi: 10.1093/nar/
 686 gkae1078.
 687

688 Jaehyun Nam, Jinsung Yoon, Jiefeng Chen, Jinwoo Shin, Sercan Ö Arik, and Tomas Pfister. Mle-
 689 star: Machine learning engineering agent via search and targeted refinement. *arXiv preprint
 690 arXiv:2506.15692*, 2025.
 691

692 Randal S Olson and Jason H Moore. Tpot: A tree-based pipeline optimization tool for automating
 693 machine learning. In *Workshop on automatic machine learning*, pp. 66–74. PMLR, 2016.
 694

695 OpenAI. Introducing chatgpt agent: Bridging research and action. <https://openai.com/index/introducing-chatgpt-agent/>, July 2025.
 696

697 Zeeshan Rasheed, Muhammad Waseem, Kai Kristian Kemell, Aakash Ahmad, Malik Abdul Sami,
 698 Jussi Rasku, Kari Systä, and Pekka Abrahamsson. Large language models for code generation:
 699 The practitioners perspective. *arXiv preprint arXiv:2501.16998*, 2025.
 700

701 Bernardino Romera-Paredes, Mohammadamin Barekatain, Alexander Novikov, Matej Balog,
 702 M Pawan Kumar, Emilien Dupont, Francisco JR Ruiz, Jordan S Ellenberg, Pengming Wang,
 703 Omar Fawzi, et al. Mathematical discoveries from program search with large language models.
 704 *Nature*, 625(7995):468–475, 2024.

702 Eui S. Seo, Sang K. Lee, and Young M. Son. Multifaceted functions of tissue-resident memory t
 703 cells in tumorigenesis and cancer immunotherapy. *Cancer Immunology, Immunotherapy*, 74(6):
 704 184, April 2025. doi: 10.1007/s00262-025-04035-x. URL <https://doi.org/10.1007/s00262-025-04035-x>.

705

706 Valentine Svensson, Sarah A Teichmann, and Oliver Stegle. Spatialde: identification of spatially
 707 variable genes. *Nature methods*, 15(5):343–346, 2018.

708

709 Yanchao Tan, Hang Lv, Yunfei Zhan, Guofang Ma, Bo Xiong, and Carl Yang. Boxlm: Unifying
 710 structures and semantics of medical concepts for diagnosis prediction in healthcare. In *Forty-
 711 second International Conference on Machine Learning*, 2025.

712

713 Xiangru Tang, Zhuoyun Yu, Jiapeng Chen, Yan Cui, Daniel Shao, Weixu Wang, Fang Wu, Yuchen
 714 Zhuang, Wenqi Shi, Zhi Huang, et al. Cellforge: Agentic design of virtual cell models. *arXiv
 715 preprint arXiv:2508.02276*, 2025.

716 InternAgent Team, Bo Zhang, Shiyang Feng, Xiangchao Yan, Jiakang Yuan, Runmin Ma, Yusong
 717 Hu, Zhiyin Yu, Xiaohan He, Songtao Huang, Shaowei Hou, Zheng Nie, Zhilong Wang, Jinyao
 718 Liu, Tianshuo Peng, Peng Ye, Dongzhan Zhou, Shufei Zhang, Xiaosong Wang, Yilan Zhang,
 719 Meng Li, Zhongying Tu, Xiangyu Yue, Wangli Ouyang, Bowen Zhou, and Lei Bai. Internagent:
 720 When agent becomes the scientist – building closed-loop system from hypothesis to verification,
 721 2025. URL <https://arxiv.org/abs/2505.16938>.

722

723 Patara Triarat, Wonyong Jeong, and Sung Ju Hwang. Automl-agent: A multi-agent llm framework
 724 for full-pipeline automl. *arXiv preprint arXiv:2410.02958*, 2024.

725

726 Renbo Tu, Nicholas Roberts, Mikhail Khodak, Junhong Shen, Frederic Sala, and Ameet Talwalkar.
 727 NAS-bench-360: Benchmarking neural architecture search on diverse tasks. In *Thirty-sixth Con-
 728 ference on Neural Information Processing Systems Datasets and Benchmarks Track*, 2022. URL
 729 <https://openreview.net/forum?id=xUXTbq6gWsB>.

730

731 David Van Dijk, Roshan Sharma, Juozas Nainys, Kristina Yim, Pooja Kathail, Ambrose J Carr, Cas-
 732 sandra Burdziak, Kevin R Moon, Christine L Chaffer, Diwakar Patabiraman, et al. Recovering
 733 gene interactions from single-cell data using data diffusion. *Cell*, 174(3):716–729, 2018.

734

735 Lukas M Weber, Arkajyoti Saha, Abhirup Datta, Kasper D Hansen, and Stephanie C Hicks. nnsvg
 736 for the scalable identification of spatially variable genes using nearest-neighbor gaussian pro-
 737 cesses. *Nature communications*, 14(1):4059, 2023.

738

739 Xu Yang, Xiao Yang, Shikai Fang, Bowen Xian, Yuante Li, Jian Wang, Minrui Xu, Haoran Pan,
 740 Xinpeng Hong, Weiqing Liu, Yelong Shen, Weizhu Chen, and Jiang Bian. R&d-agent: Automat-
 741 ing data-driven ai solution building through llm-powered automated research, development, and
 742 evolution, 2025. URL <https://arxiv.org/abs/2505.14738>.

743

744 Jiakang Yuan, Xiangchao Yan, Shiyang Feng, Bo Zhang, Tao Chen, Botian Shi, Wanli Ouyang,
 745 Yu Qiao, Lei Bai, and Bowen Zhou. Dolphin: Moving towards closed-loop auto-research through
 746 thinking, practice, and feedback, 2025. URL <https://arxiv.org/abs/2501.03916>.

747

748 Ke Zhang, Wanwan Feng, and Peng Wang. Identification of spatially variable genes with graph cuts.
 749 *Nature Communications*, 13(1):5488, 2022a.

750

751 Martin Jinye Zhang, Kangcheng Hou, Kushal K Dey, Saori Sakaue, Karthik A Jagadeesh, Kathryn
 752 Weinand, Aris Taychameekiatchai, Poorvi Rao, Angela Oliveira Pisco, James Zou, et al. Poly-
 753 genic enrichment distinguishes disease associations of individual cells in single-cell rna-seq data.
 754 *Nature genetics*, 54(10):1572–1580, 2022b.

755

756 Yuqing Zhang, Giovanni Parmigiani, and W Evan Johnson. Combat-seq: batch effect adjustment
 757 for rna-seq count data. *NAR genomics and bioinformatics*, 2(3):lqaa078, 2020.

758

759 Zijun Zhang, Christopher Y Park, Chandra L Theesfeld, and Olga G Troyanskaya. An automated
 760 framework for efficiently designing deep convolutional neural networks in genomics. *Nature
 761 Machine Intelligence*, 3(5):392–400, 2021.

756 Jian Zhou and Olga G Troyanskaya. Predicting effects of noncoding variants with deep learning–
757 based sequence model. *Nature methods*, 12(10):931–934, 2015.
758

759 Jiaqiang Zhu, Shiquan Sun, and Xiang Zhou. Spark-x: non-parametric modeling enables scalable
760 and robust detection of spatial expression patterns for large spatial transcriptomic studies. *Genome*
761 *biology*, 22(1):184, 2021.

762
763
764
765
766
767
768
769
770
771
772
773
774
775
776
777
778
779
780
781
782
783
784
785
786
787
788
789
790
791
792
793
794
795
796
797
798
799
800
801
802
803
804
805
806
807
808
809

810
811
812
A ALGORITHM TABLE

813 Symbol	814 Type	815 Description
\mathcal{T}	Task description	Short description of task (e.g., single-cell RNA-seq imputation).
\mathcal{D}	Dataset	Data used in running the method.
$h(\cdot)$	Evaluator	Scoring function that maps a solution s to a scalar performance score.
s_{init}	Initial solution (optional)	Optional user-provided initial solution to start from.
T_{budget}	Time budget	Maximum wall-clock time allowed for the optimization loop (default: 8 hours).
A_{paper}	Subroutine	“Paper agent”: retrieves and summarizes domain-relevant literature given \mathcal{T} .
\mathcal{P}	Set of documents	Domain knowledge / paper summaries collected by $A_{\text{paper}}(\mathcal{T})$.
A_{cate}	Subroutine	Agent that proposes high-level instruction categories for solving \mathcal{T} .
$\text{DraftThenRefine}(\cdot)$	Procedure	Drafting–refinement procedure used to iteratively improve structured text (categories or instructions).
\mathcal{C}	Set	Set of instruction categories (e.g., preprocessing, noise modeling, model architecture, etc.).
$\{\pi_c\}_{c \in \mathcal{C}}$	Probabilities	Categorical distribution over categories \mathcal{C} , encoding their estimated usefulness.
c	Category index	Individual category element from \mathcal{C} .
A_{instr}	Subroutine	Agent that drafts and refines concrete instructions for a specific category c .
\mathcal{I}_c	Set of instructions	Category-specific instructions for optimizing solutions under category c .
\mathcal{F}_c	Feedback set	Collected feedback specific to category c .
$\mathcal{I}_{\text{diag}}$	Instructions	Diagnostic instructions describing how to print informative method information.
$\mathcal{F}_{\text{diag}}$	Feedback set	Feedback collected from diagnostic runs.
A_{init}	Subroutine	Agent that generates initial candidate solutions using \mathcal{T} , \mathcal{P} , and s_{init} .
\mathcal{S}	Solution set	Current pool / archive of candidate solutions explored so far.
N_{top}	Integer	Number of top diverse solutions selected from \mathcal{S} at each iteration.
s	Solution	A single candidate solution sampled from the current top set.
α	Scalar probability	Probability of using instruction-based optimization instead of diagnostic-based optimization (default: 0.8).
$\text{Bernoulli}(\alpha)$	Distribution	Stochastic decision: with probability α use instruction-based optimization; otherwise use diagnostics.
$\text{Cat}(\{\pi_c\}_{c \in \mathcal{C}})$	Distribution	Categorical distribution over categories \mathcal{C} parameterized by $\{\pi_c\}$.
A_{optim}	Subroutine	Agent that improves a solution s using instructions \mathcal{I}_c and feedback \mathcal{F}_c .
s'	Solution	New candidate solution obtained by optimizing s .
A_{feedback}	Subroutine	Agent that analyzes the change from s to s' and produces textual feedback.
A_{diag}	Subroutine	Diagnostic agent that uses data \mathcal{D} and diagnostic info $(\mathcal{I}_{\text{diag}}, \mathcal{F}_{\text{diag}})$ to improve s .
N_{sol}	Integer	Adjusted number of solutions to keep / explore in future rounds (e.g., $N_{\text{sol}} = \max(1, N_{\text{top}} - 1)$).
s^*	Solution	Best-found solution at the end of the run, i.e., $s^* \in \arg \max_{s \in \mathcal{S}} h(s)$.
wall-clock time	Time	Actual elapsed real-world time since the algorithm started.

858
859
860
861
862
863
Table 4: Explanation of symbols and subroutines used in Algorithm 1.

864 B EXAMPLE TUSOAI CODE TEMPLATE

866

Single-cell denoising template file

```
869
870     import scanpy as sc
871     import pandas as pd
872     import numpy as np
873     import scipy as sp
874     import magic
875     from anndata import read_h5ad
876     import scprep
877     from scipy.sparse import csr_matrix
878     from sklearn.neighbors import NearestNeighbors
879     from scipy.sparse import issparse
880     from sklearn.decomposition import PCA
881     from anndata import AnnData
882     import random
883
884     def mse(adata):
885         import anndata
886         import scanpy as sc
887         import scprep
888         import sklearn.metrics
889
890         test_data = anndata.AnnData(X=adata.obs["test"], obs=adata.obs, var=adata.var)
891         denoised_data = anndata.AnnData(
892             X=adata.obs["denoised"], obs=adata.obs, var=adata.var
893         )
894
895         # scaling and transformation
896         target_sum = 10000
897
898         sc.pp.normalize_total(test_data, target_sum=target_sum)
899         sc.pp.log1p(test_data)
900
901         sc.pp.normalize_total(denoised_data, target_sum=target_sum)
902         sc.pp.log1p(denoised_data)
903
904         error = sklearn.metrics.mean_squared_error(
905             scprep.utils.toarray(test_data.X), denoised_data.X
906         )
907         return error
908
909     def tuso_model(adata):
910
911         adata.obs["denoised"] = ...
912         return adata
913
914     def main():
915         np.random.seed(42)
916         random.seed(42)
917         adata = read_h5ad('openproblems_datasets/1k_pbmc_processed.h5ad')
918         print("tuso_model_start")
919         adata = tuso_model(adata)
920         print("tuso_model_end")
921
922         val_metric = 1 - mse(adata)
923         print(f"tuso_evaluate: {val_metric}")
924
925     main()
926
927
928
929
930
931
932
933
934
935
936
937
938
939
940
941
942
943
944
945
946
947
948
949
950
951
952
953
954
955
956
957
958
959
960
961
962
963
964
965
966
967
968
969
970
971
972
973
974
975
976
977
978
979
980
981
982
983
984
985
986
987
988
989
990
991
992
993
994
995
996
997
998
999
999
```

918
919

C EXAMPLE INSTRUCTIONS GENERATED BY TUSOAI

920
921**Example categories for single-cell denoising**922
923

- data_preprocessing
- feature_engineering
- model_architecture
- hyperparameter_tuning
- imputation_strategies
- normalization_methods
- evaluation_metrics
- cross_validation
- domain_knowledge_integration
- robustness_techniques
- noise_modeling
- dropout_probability_estimation
- graph_neural_network_optimization
- dropout_pattern_analysis
- pipeline_interaction_analysis
- low_rank_approximation_optimization
- autoencoder_classifier_integration

924
925926
927928
929930
931932
933934
935936
937938
939940
941942
943944
945**Example instructions within a category**946
947948
949950
951952
953954
955956
957958
959960
961962
963964
965966
967968
969970
971

- leveraging graph attention mechanisms to focus on informative cell interactions
- incorporating multi-layer graph convolutions to capture hierarchical gene expression patterns
- implementing edge dropout to enhance model robustness against noise in cell relationships
- utilizing message passing to propagate information across similar cell types effectively
- integrating adaptive learning rates for different graph nodes based on local connectivity
- employing graph pooling techniques to summarize cellular features without losing critical information
- applying graph regularization to maintain structural integrity of the cellular network
- utilizing node embeddings to capture latent features of gene expression profiles
- optimizing neighborhood sizes dynamically based on data density in the graph
- exploring higher-order graph structures to uncover complex relationships in RNA-seq data

972
973

C.1 PREDEFINED DIAGNOSTIC INSTRUCTIONS

974
975**Example predefined diagnostic instructions**976
977

- altering or adding diagnostic information to be printed
- altering or adding complex diagnostic information of specific model components
- printing key statistical assumptions underlying the model (e.g., independence, normality)
- emitting warnings when model assumptions appear to be violated by the data
- logging all implicit assumptions made during model selection or preprocessing
- printing assumptions related to feature distributions or transformations
- displaying model-specific assumptions such as linearity, homoscedasticity, or no multicollinearity
- printing assumptions about data completeness, such as missing value tolerance
- logging expectations about input feature scaling or normalization
- displaying prior distributions or regularization beliefs embedded in the model
- printing assumptions about label distribution (e.g., class balance or stratification)
- emitting diagnostics when data fails to meet i.i.d. assumptions
- logging assumed causal directions or conditional independencies in the model
- printing constraints assumed on feature ranges or valid input domains
- warning if assumptions about sufficient training data volume are not met
- displaying structural assumptions, such as sparsity or low-rank representations
- logging assumptions related to stationarity or autocorrelation in time-dependent data

999

1000

1001

1002

1003

1004

1005

1006

1007

1008

1009

1010

1011

1012

1013

1014

1015

1016

1017

1018

1019

1020

1021

1022

1023

1024

1025

1026 **D SINGLE-CELL ANALYSIS TASKS SETUP**
1027
1028

1029 The OpenProblems benchmark (Luecken et al., 2025) contains 12 single-cell analysis tasks with
1030 numerous testing datasets and benchmark metrics for each. We select 6 tasks: single-cell denoising,
1031 label projection, batch integration, spatially variable gene identification, spatial decomposition of
1032 cell types, and visualization. These were selected with the following criteria. First, we required
1033 more than one dataset, such that we can optimize on one dataset, and deploy the learned method
1034 on the remaining testing datasets, excluding the 2 cell-cell communication tasks and perturbation
1035 prediction. Second, a publicly available Github to ensure we are reproducing the testing procedures
1036 correctly, excluding multimodal integration and modality prediction. Third, a method for the task
1037 should be able to run in a reasonable amount of time on a CPU, excluding the foundation model
1038 benchmark.

1039 In each task, we performed optimization on one dataset which could be run in a reasonable amount
1040 of time (< 2 minutes for a simple baseline model). The learned methods of each baseline were
1041 then applied to the deployment datasets. In selecting benchmark metrics for each task, we had three
1042 criteria. First, the metric should not have unavoidable trivial solutions, excluding the Poisson loss
1043 metric from denoising, as this can be easily minimized by simply down-weighting lowly expressed
1044 genes, including by just scaling genes by their variance or re-normalizing the data. Second, the
1045 metrics should be computationally efficient to run, so optimization speed of each method will not
1046 be dominated by running metrics. This excluded several metrics from batch integration and visual-
1047 ization. Third, the metric should line up with the task. In the SVG task, it is initially measured in
1048 correlation with spatial variability scores, however, the simulation procedure generates binary 0/1
1049 labels of spatial variability, thus we use accuracy of classifying a gene as SVG instead. We also nor-
1050 malize metrics such that each is between 0 and 1 and a higher score is better. The score in denoising
1051 is 1-MSE, normalized so that no denoising is 0, and perfect denoising is 1. The score in spatial
1052 decomposition is normalized so that a random cell type assignment is 0, and perfect decomposition
1053 is 1. See Table 5 for a full breakdown of datasets and metrics used in single-cell tasks.
1054

	Optimization dataset	Testing datasets	Benchmark metrics
Denoise	1K PBMC	5K PBMC Pancreatic	MSE
Label	5k cells from Immune Cell Atlas	Diabetic Kidney GTEx v9 HypoMap Mouse Pancreatic Islet Atlas Tabula Sapiens	Accuracy F1 macro F1 micro F1 weighted
Batch	5k cells from Immune Cell Atlas	Diabetic Kidney GTEx v9 HypoMap Mouse Pancreatic Islet Atlas Tabula Sapiens	Graph connectivity ASW label ASW batch
SVG	Drosophila Stereo-seq E5	Drosophila Stereo-seq E10 Drosophila Stereo-seq E9 Drosophila Stereo-seq E6	Accuracy
Decomp	TMS Lung (alpha=1.0)	TMS Lung (alpha=0.5) TMS Lung (alpha=5.0) Pancreas (alpha=0.5) Pancreas (alpha=1.0) Pancreas (alpha=5.0)	R^2
Visual	Mouse HSPCT	5K PBMC Mouse Myeloid Zebrafish	Trustworthiness Distance correlation Density Preservation

1076 **Table 5: Single-cell benchmark setup.** Datasets and metrics refer to the setup on the OpenProblems
1077 webpage.
1078

1080 E DEEP LEARNING TASKS SETUP
10811082 The NASBENCH-360 benchmark Tu et al. (2022) contains 10 deep learning tasks across scientific
1083 domains with predefined training, validation, and testing splits, as well as evaluation procedures.
1084 We select 5 tasks: Spherical, NinaPro, DeepSEA, Satellite, and ECG. These were selected with the
1085 following criteria. First, the task should be scientific and somewhat understudied compared to stan-
1086 dard ML tasks, excluding the 2 standard image and audio classification tasks. Second, to ensure fair
1087 comparison against the precomputed baselines, we removed tasks where we were uncertain about
1088 reproducing the evaluation procedure, partly due to recent GitHub or package updates requiring
1089 debugging, excluding Cosmic, PSICOV, and DarcyFlow.1090 In each task, we performed optimization by training a model on the predefined training set and
1091 attaining a score on the validation set. The final testing accuracy of optimized models is attained
1092 when deploying the model on the predefined test set. We use the same splits and metrics defined in
1093 the original paper.1094
1095
1096
1097
1098
1099
1100
1101
1102
1103
1104
1105
1106
1107
1108
1109
1110
1111
1112
1113
1114
1115
1116
1117
1118
1119
1120
1121
1122
1123
1124
1125
1126
1127
1128
1129
1130
1131
1132
1133

1134 F BASELINE IMPLEMENTATIONS

1135

1136 **AIDE.** AIDE takes as input a data folder, task description, and evaluation metric. While originally
 1137 designed for whole-workflow construction in ML tasks, this can be adapted to general optimization
 1138 in the following ways. First, AIDE can operate on any data input in the data folder. If specific
 1139 preprocessing information was needed, we could input this code to the task description. Second,
 1140 in place of specifying an accuracy metric (e.g., "F1 score"), we instead simply input the entire
 1141 evaluation function in Python, and found this worked well. As our goal is optimization and not
 1142 construction, AIDE's initial prompt is tuned until code was consistently generated and optimized
 1143 upon, typically requiring the same formatting information as other methods. AIDE is run for the
 1144 same length as TussoAI (8 hours) in the same conda environment on the same CPU (Optimization
 1145 for AIDE and TussoAI is performed on the same Intel(R) Xeon(R) Gold 5416S.) or GPU (Intel(R)
 1146 Xeon(R) Silver 4314 CPU @ 2.40GHz), given 4 threads and 50GB of memory. While AIDE does
 1147 have a default timeout per execution of 1 hour, on attempting to set this to the same time as TussoAI
 1148 led to consistent crashes on more than half of tasks, thus we left it as is.

1149 **Biomni.** We access Biomni through its web page. Biomni runs on a CPU and can take input files
 1150 up to a limit, has a runtime execution of 1 hour per iteration. While not specifically designed for
 1151 optimization, we can upload the same template code and data as TussoAI then ask Biomni to perform
 1152 an iterative process of updates. In practice, this led to between 2 and 10 iterations per task between
 1153 20 minutes and 4 hours. This procedure was signed off by the original authors of Biomni.

1154 **ChatGPT-Agent.** We access ChatGPT-Agent through its web page. ChatGPT-Agent can accept
 1155 input files up to 25MB and has a runtime execution of 1 hour per iteration. We upload the same
 1156 template code and data as TussoAI and ask ChatGPT-Agent to perform an iterative process of updates.
 1157 In practice, this led to between 2 and 7 iterations per task between 10 minutes and 5 hours.

1158 **Expert.** The expert baselines for NASBench-360 are pre-computed from their paper. The original
 1159 authors found the best performing expert models from the literature for each task. This includes the
 1160 following methods:

1161

- 1162 1. DeepSea - The original DeepSea model released alongside the dataset, a 1D convolution
 1163 model with state of the art performance. (Zhou & Troyanskaya, 2015)
- 1164 2. NinaPro - Feed-forward neural network with attention modules in place of convolutions.
 1165 (Josephs et al., 2020)
- 1166 3. Spherical - a spherical CNN with special operations for spherical signals. This model
 1167 achieved state of the art performance on spherical MNIST. (Cohen et al., 2018)
- 1168 4. Satellite - A linear classifier with convolution kernel as feature extractor, achieving state of
 1169 the art on UCR time series prediction tasks. (Dempster et al., 2020)
- 1170 5. ECG - ResNet with 1D convolution, achieving state of the art on several time series predic-
 1171 tion tasks for medicine. (Hong et al., 2020)

1173 For single-cell tasks, we selected the expert method with the following criteria. First, it should
 1174 be within the top 3 methods as defined by the existing OpenProblems benchmarking. Second, the
 1175 OpenProblems Github should have code for reproducing this method. Third, we selected the method
 1176 that was particularly efficient compared to others, if applicable, defined by a runtime of less than 10
 1177 minutes on OpenProblems, with others having greater than 1 hour. This left us with the following
 1178 expert methods, whose code we extracted from the OpenProblems Github:

1180

- 1181 1. Denoise – MAGIC, a graph-based diffusion method that imputes missing gene expression
 1182 values. (Van Dijk et al., 2018)
- 1183 2. Batch – ComBat, an empirical Bayes approach that removes batch effects across samples.
 1184 (Zhang et al., 2020)
- 1185 3. Label – PCA + Logistic Regression, which uses low-dimensional PCs as features for effi-
 1186 cient cell-type classification. (Luecken et al., 2025)
- 1187 4. Decomposition – NNLS, a non-negative least squares model for estimating gene programs
 1188 or latent factors. (Aliee & Theis, 2021)

1188 5. SVG – SPARK-X, a spatial variance component model that identifies spatially variable
1189 genes at scale. (Zhu et al., 2021)
1190 6. Visualize – t-SNE (log10CP10K), a nonlinear embedding of log-transformed counts for 2D
1191 visualization. (Luecken et al., 2025)
1192

1193 **Claude-4-Sonnet and GPT-5.** In deep learning tasks where Biomni and ChatGPT-Agent cannot
1194 apply due to computational limitations (file size, runtime, GPU access), we substitute the best of
1195 10 models generated by Claude-4-Sonnet and GPT-5. 10 models are generated by prompting these
1196 LLMs using the same template that would have been used in Biomni and ChatGPT-Agent. The best
1197 is decided by the top performing model on the validation dataset which ran in less than one hour,
1198 akin to the runtime limitations of Biomni and ChatGPT-Agent.

1199
1200
1201
1202
1203
1204
1205
1206
1207
1208
1209
1210
1211
1212
1213
1214
1215
1216
1217
1218
1219
1220
1221
1222
1223
1224
1225
1226
1227
1228
1229
1230
1231
1232
1233
1234
1235
1236
1237
1238
1239
1240
1241

1242 **G EXAMPLE TASK INFORMATION**
1243

	Denoise
1245	Task Description
1246	single cell RNA-seq imputation
1247	Drafted Categories
1248	data_normalization feature_selection imputation_modeling latent_space_representation noise_handling batch_effect_correction hyperparameter_tuning evaluation_metrics ensemble_imputation_methods domain_specific_constraints count_distribution_modeling
1249	Refined Categories
1250	data_normalization feature_selection imputation_modeling latent_space_representation noise_handling batch_effect_correction hyperparameter_tuning evaluation_metrics ensemble_imputation_methods domain_specific_constraints count_distribution_modeling dropout_probability_estimation graph_based_representation dropout_pattern_analysis pipeline_interaction_analysis rank_estimation_and_optimization virtual_class_label_generation
1251	Drafted Solution Descriptions
1252	k-nearest neighbors imputation matrix factorization (e.g., PCA, NMF) autoencoder-based imputation (including DCA) generative adversarial networks (GANs) for imputation deep learning models (e.g., U-Net architecture)
1253	Refined Solution Descriptions
1254	k-nearest neighbors imputation matrix factorization (e.g., PCA, NMF) autoencoder-based imputation (including DCA) deep learning models (e.g., U-Net architecture) graph neural network (GNN) for imputation scImpute for dropout imputation co-occurrence clustering based on dropout patterns scran normalization with prior clustering AutoClass model for scRNA-Seq cleaning low-rank matrix approximation (ALRA)

1292
1293
1294
1295

1296 H NOVELTY OF DISCOVERED METHODS

1298 For the four example methods constructed by TusoAI listed in Section 4.1, we expand on the novelty
 1299 claim with a thorough literature review of related methods.

1300 In single-cell denoise, TusoAI designed a non-negative matrix factorization (NMF) approach that
 1301 models dropout rates, Poisson noise, and performs iterative refinement, distinct from the only other
 1302 NMF-based approach in the OpenProblems benchmark, ALRA (Linderman et al., 2022). Specif-
 1303 ically, ALRA applies a low-rank approximation to a globally normalized matrix and performs an
 1304 adaptive thresholding step to restore zeros, but it does not explicitly model count noise, does not
 1305 incorporate dropout mechanisms, and does not iteratively refine factors. Another denoising method
 1306 uses NMF, DenoiseIt (Jeon et al., 2024). This method focuses on identifying noisy features via
 1307 NMF loadings combined with isolation-forest filtering, and does not perform probabilistic mod-
 1308 eling of gene-cell counts or imputation of dropout-affected expression values, again distinct from
 1309 our approach. Another point of novelty is that TusoAI’s learned method is outperforming MAGIC
 1310 (Van Dijk et al., 2018), which was found to outperform ALRA (Luecken et al., 2025).

1311 In SVG, TusoAI adapted known techniques such as modeling expression as a function of spatial co-
 1312 ordinates and neighborhood summaries to create a custom, high-performing method. Many existing
 1313 SVG detectors are primarily coordinate-based, using Gaussian-process or generalized linear models
 1314 over spatial locations (SpatialDE, SpatialDE2, SPARK-X, GPcounts, BOOST-GP) (Svensson et al.,
 1315 2018; Kats et al., 2021; Zhu et al., 2021; BinTayyash et al., 2021; Li et al., 2021), while others rely
 1316 mainly on neighborhood or graph structure, diffusion, or spatial autocorrelation statistics (Moran’s
 1317 I, SOMDE, scGCO, Sepal, SpaGCN, SpaGFT, nnSVG, Spanve) (Luecken et al., 2025; Hao et al.,
 1318 2021; Zhang et al., 2022a; Andersson & Lundeberg, 2021; Hu et al., 2021; Chang et al., 2024; Weber
 1319 et al., 2023; Cai et al., 2023). Graph-based models such as SpaGCN and SpaGFT can incorporate
 1320 both spatial coordinates and local neighborhoods through graph constructions and convolution or
 1321 spectral transforms (Hu et al., 2021; Chang et al., 2024), but they do not explicitly combine smooth
 1322 coordinate regression with fixed neighborhood summary covariates in a single per-gene predictive
 1323 model as TusoAI does. This joint modeling of coordinate trends and neighborhood summaries en-
 1324 ables TusoAI to outperform SPARK-X (Zhu et al., 2021) on our SVG benchmark, despite SPARK-X
 1325 being among the strongest existing SVG baselines (Luecken et al., 2025).

1326 In Satellite, TusoAI combined preprocessing, training procedures, loss functions, and ensembling
 1327 techniques to build the top-performing model. First, this is distinct from the expert model, which is
 1328 a linear classifier (Dempster et al., 2020). Second, these kinds of pipeline-level decisions lie outside
 1329 the search space of the NAS baselines used in NASBench-360: methods such as DARTS-GAEA,
 1330 DenseNAS, AMBER, and tuned WRN search only over convolutional architectures under a fixed
 1331 data preprocessing pipeline, standard loss, and a single-model training recipe, and therefore cannot
 1332 automatically implement the techniques TusoAI does here.

1333 In Spherical, TusoAI fine-tuned layers of ResNet-50 and augmented the data with random flips and
 1334 rotations. First, this is distinct from the expert model, which is a spherical CNN (Cohen et al., 2018).
 1335 Again, these decisions, such as fine-tuning Resnet-50 or augmenting data with rotations and flips lie
 1336 outside the search space for NAS methods.

1337
 1338
 1339
 1340
 1341
 1342
 1343
 1344
 1345
 1346
 1347
 1348
 1349

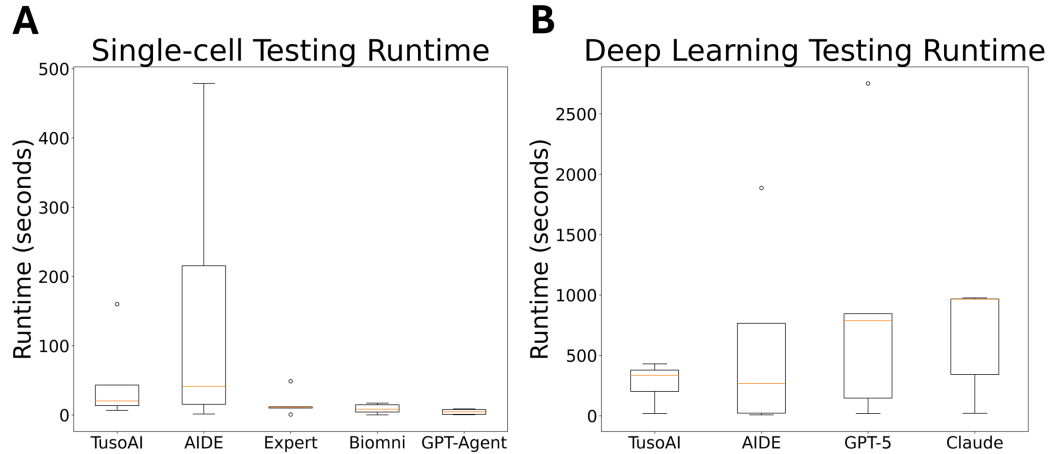
1350 I RUNTIME OF NEW METHODS
1351
1352
1353
1354
1355
1356
1357
1358
1359
1360
1361
1362
1363
1364
1365
1366
1367
1368
1369
1370
1371
1372
1373
1374
1375
1376
1377
1378
1379
1380
1381
1382
1383
1384
1385
1386
1387
1388
1389
1390
1391
1392
1393
1394
1395
1396
1397
1398
1399
1400
1401
1402
1403

Figure 5: Testing set runtime for (A) single-cell tasks (averaged over 3 random data splits) and (B) deep learning tasks (averaged over 3 random seeds).

J OPTIMIZATION TRAJECTORIES

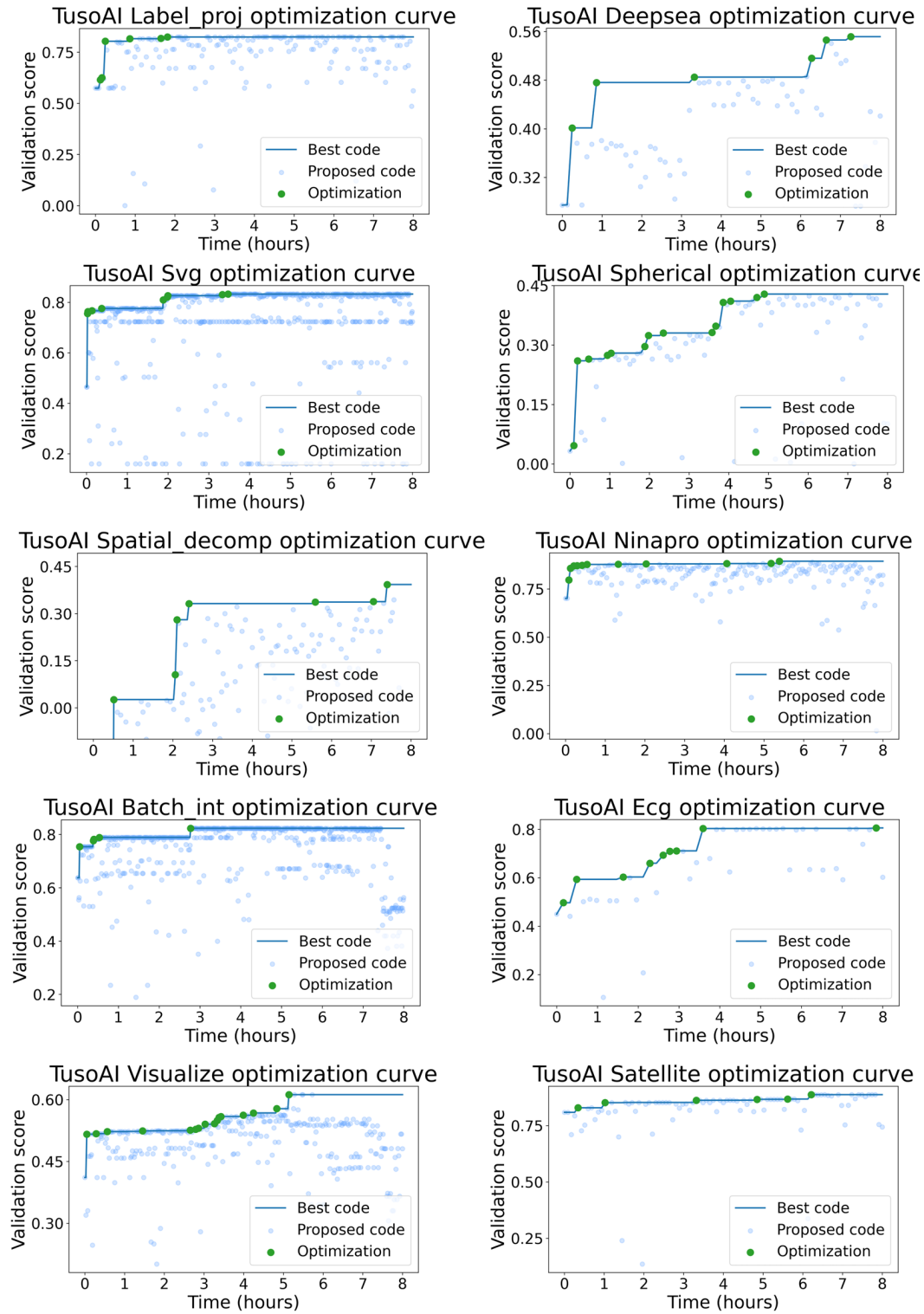
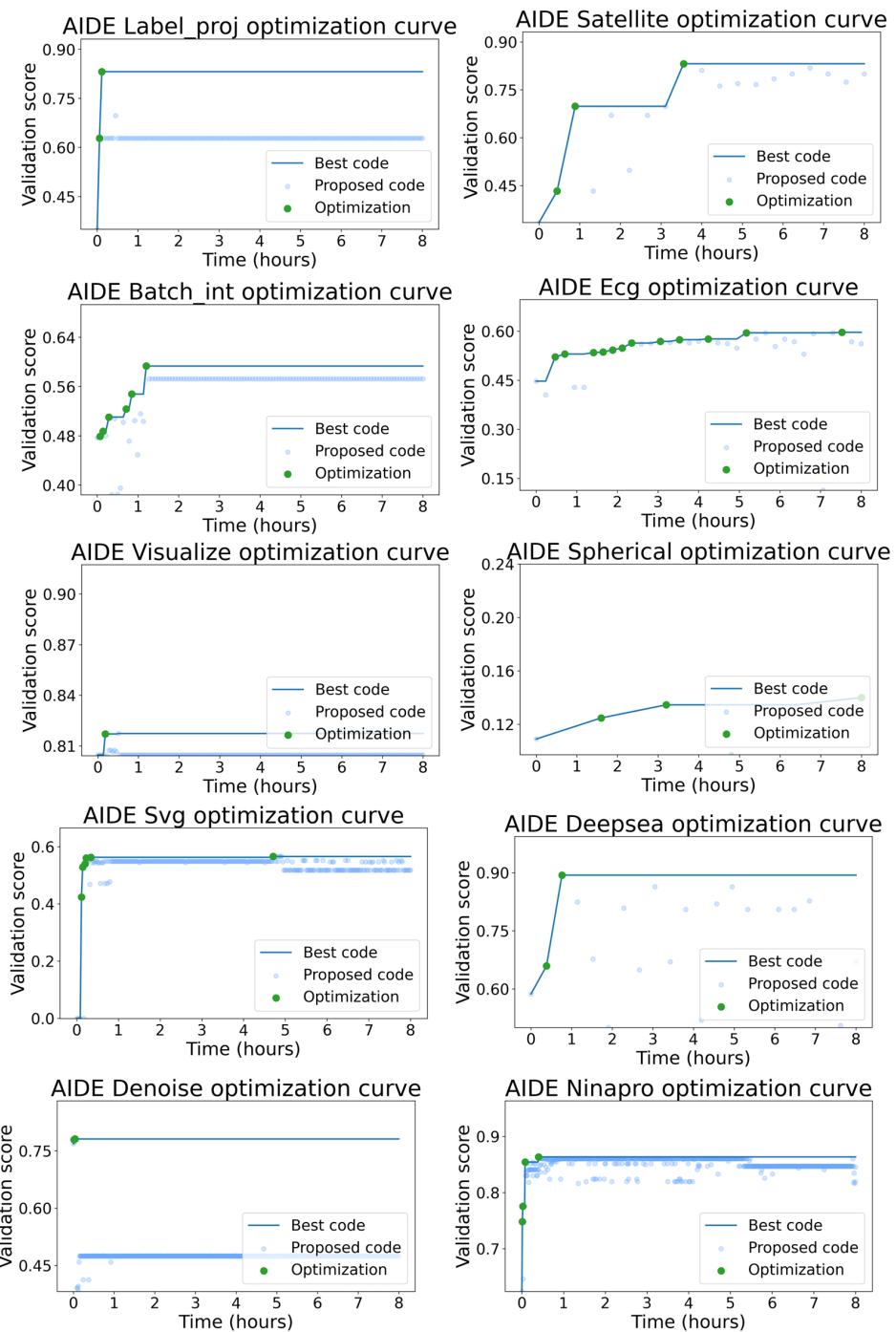


Figure 6: TusoAI’s optimization trajectory for all benchmarking tasks. Denoise is in Figure 2.

1458 K AIDE OPTIMIZATION TRAJECTORIES
1459
14601506 Figure 7: AIDE's optimization trajectory for all benchmarking tasks. AIDE can edit the evaluation
1507 function, which occurred in the decomposition task which was thus excluded.
1508
1509
1510
1511

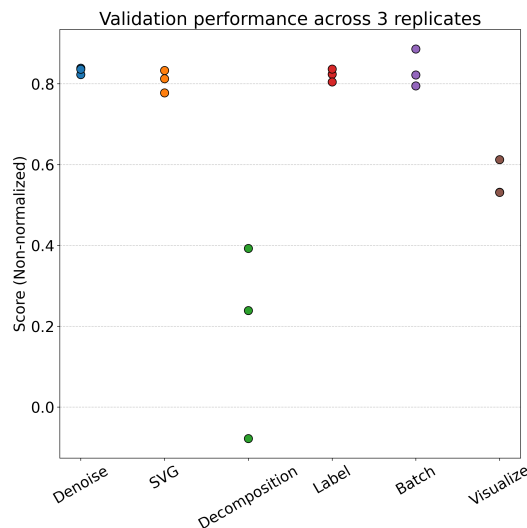
1512 L STABILITY ACROSS REPLICATES
1513

Figure 8: **Validation performance across 3 replicates.** Final validation performance after running TusooAI 3 separate times on each single-cell task.

1566
1567

M CODE DIVERSITY

1568
1569
1570
1571
1572
1573
1574
1575
1576
1577
1578

We measure the diversity of generated code, as measured by the cosine similarity of the text embedding of one generated code versus all others, similar to (Aygün et al., 2025). This is performed for TusoAI and AIDE. For each, we first filter out repetitive/uninformative code strings, including comments, imports, evaluation functions and data loading procedures (which will not change over iterations). We then apply sklearn’s TfidfVectorizer function to each cleaned code to obtain a text embedding. We can then compute the cosine similarity between pairs of code. Diversity is measured as 1-cosine similarity. We opt for TF-IDF instead of more sophisticated methods like CodeBERT (Feng et al., 2020) which measure semantic similarity, as we observed this overestimated the similarity between code (all cosine similarity > 0.997 for all tasks). This is likely due to each iteration always being a slight permutation of the same python method performing the same task. TF-IDF better captures a measure of difference between algorithmic procedures in this case.

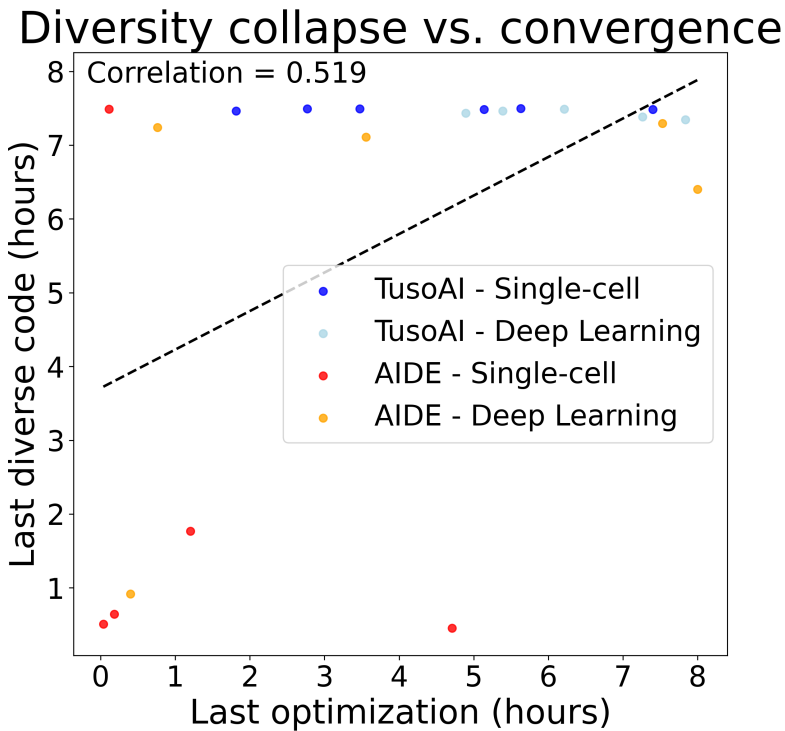
1579
1580
1581
1582
1583
1584
1585
1586
1587
1588
1589
1590
1591
1592
1593
1594
1595
1596
1597
1598
1599
1600
1601
1602
1603
1604
1605
1606
1607
1608
1609
1610
1611
1612
1613
1614
1615
1616
1617
1618
1619

Figure 9: **Code diversity versus optimization ability.** Last diverse code for each trajectory (defined as last position with diversity > 0.1) versus last optimization position.

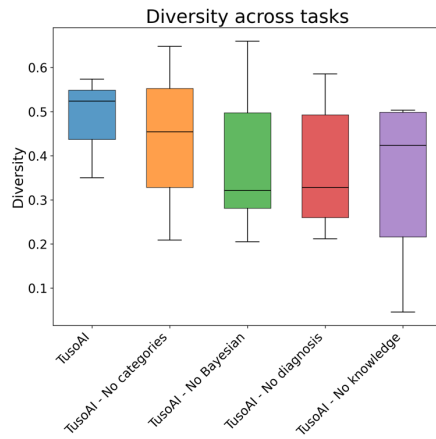
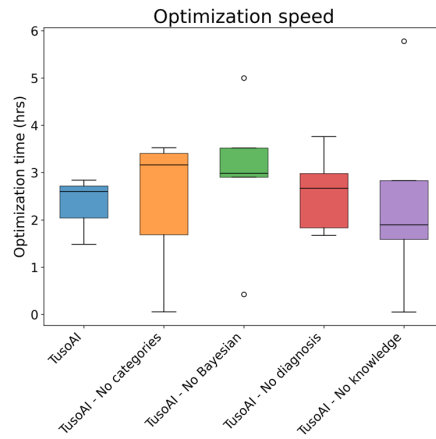
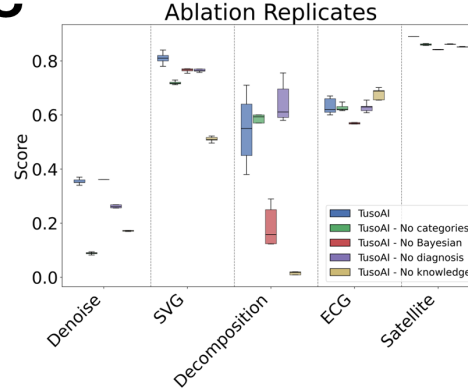
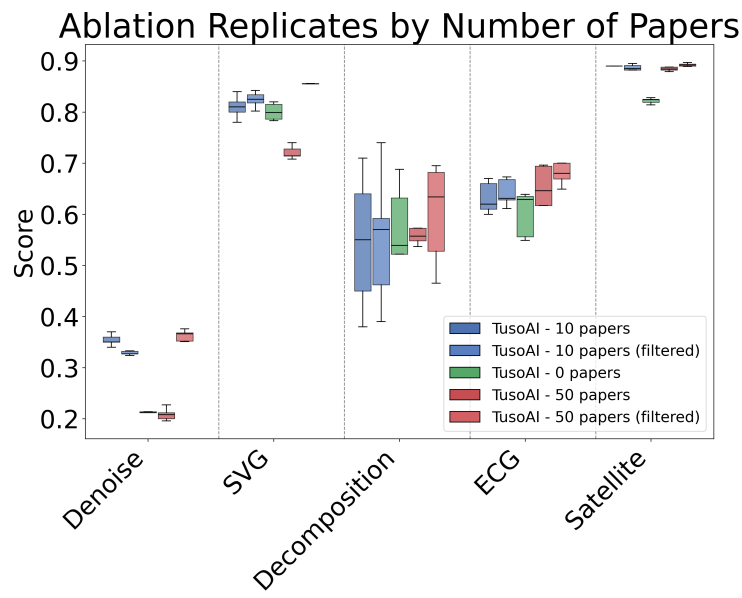
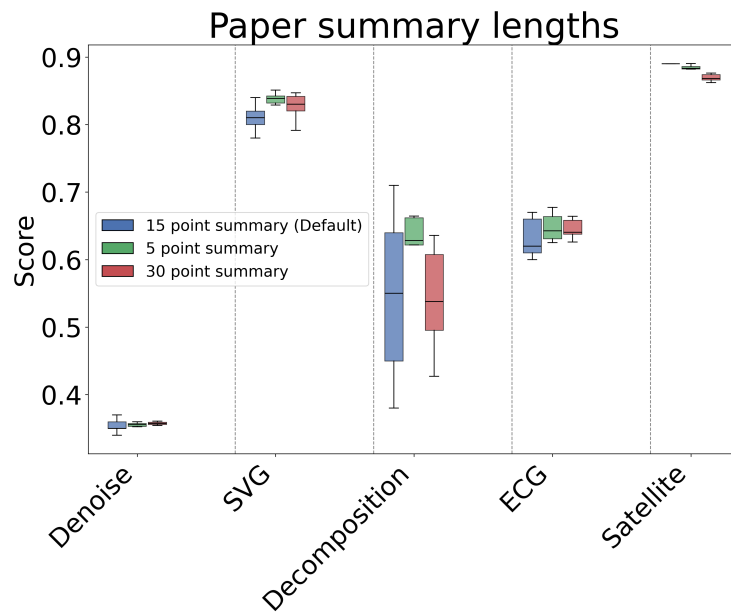
1620 N ABLATION ANALYSIS
1621
16221623
1624**A****B****C**

Figure 10: **Additional ablation information.** (A) Box plot across 5 tasks of the mean code diversity. (B) Box plot across 5 tasks of the mean time to optimize. (C) Box plot of the final testing scores of 5 replicates for each ablation.

1674 O VARYING LITERATURE SEARCHED
1675
1676
1677
1678
1679
1680
1681
1682
1683
1684
1685
1686
1687
1688
1689
1690
1691
1692
1693
1694
16951696 Figure 11: Box plot of the final testing scores of 5 replicates for collecting 10 papers (default), 0
1697 papers, and 50 papers, alongside optional paper summary filtering step.
16981700
1701
1702
1703
1704
1705
1706
1707
1708
1709
1710
1711
1712
1713
1714
1715
1716
1717
1718
1719
1720 Figure 12: Box plot of the final testing scores of 5 replicates for having 15 bullet point summaries
1721 (default), 5 bullet point summaries, and 30 bullet point summaries.
1722
1723
1724
1725
1726
1727

1728
1729
1730

P LLM ANALYSIS

1731

1732

1733

1734

1735

1736

1737

1738

1739

1740

1741

1742

1743

1744

1745

1746

1747

1748

1749

1750

1751

1752

1753

1754

1755

1756

1757

1758

1759

1760

1761

1762

1763

1764

1765

1766

1767

1768

1769

1770

1771

1772

1773

1774

1775

1776

1777

1778

1779

1780

1781

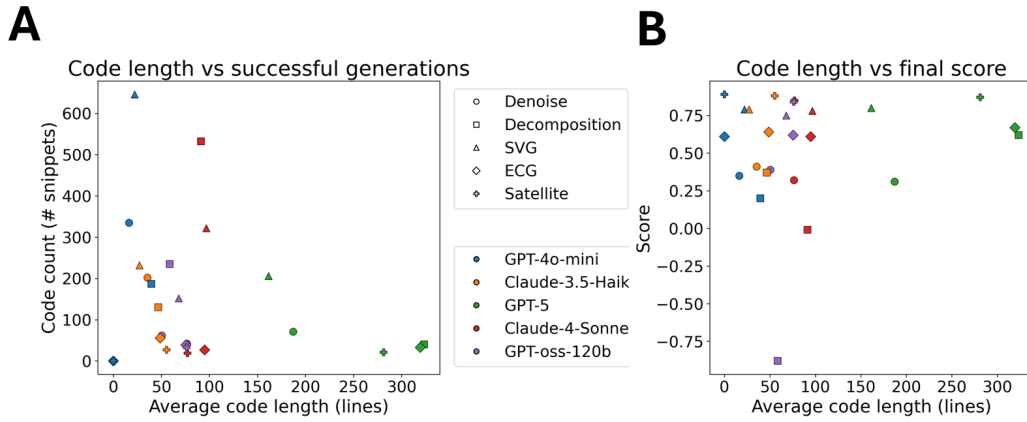
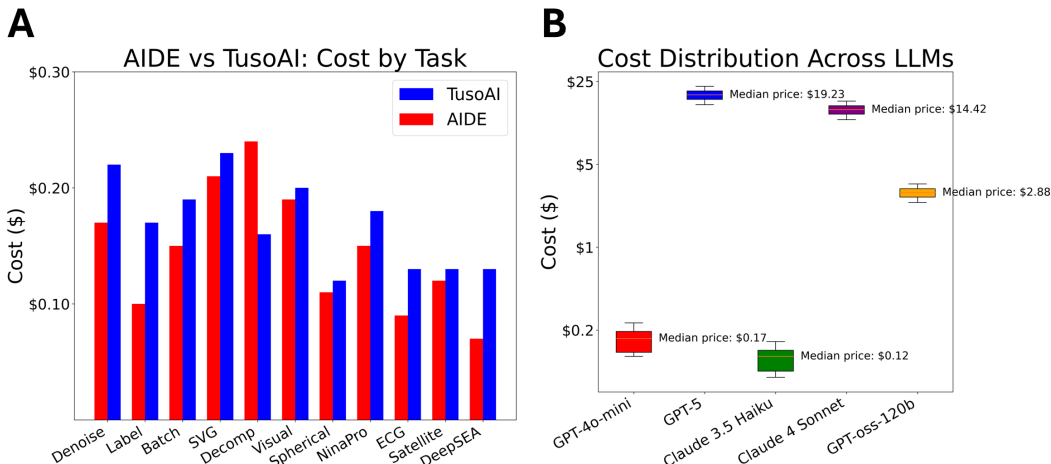


Figure 13: **Additional LLM information.** (A) Average length of generated methods for each task and LLM versus the total count of how many methods were generated. (B) Average length of generated methods for each task and LLM versus the final deployment performance.

1782
1783 **Q COST ANALYSIS**
1784
1785
1786
1787
1788
1789
1790
1791
1792
1793
1794
1795
1796
1797
1798
1799
1800
1801

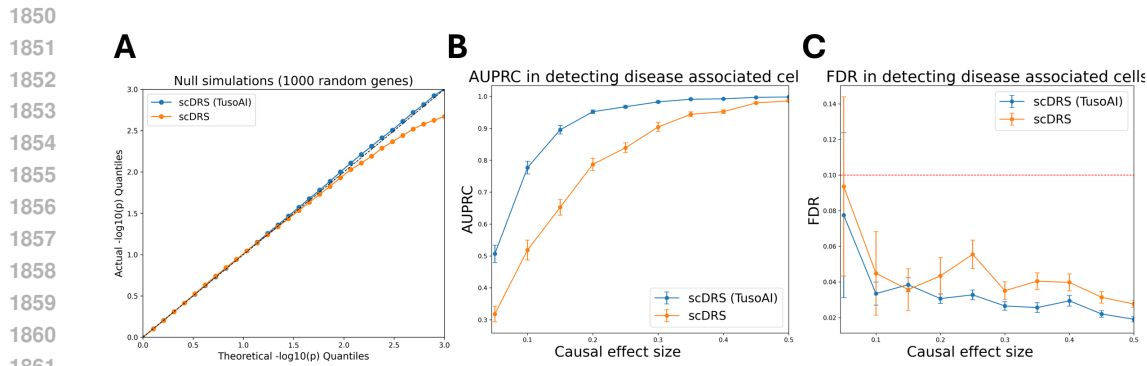
1802 **Figure 14: Cost distribution.** (A) TusoAI vs. AIDE cost for each task. (B) Boxplot of costs for
1803 each LLM on 5 ablation tasks.

1804
1805
1806
1807
1808
1809
1810
1811
1812
1813
1814
1815
1816
1817
1818
1819
1820
1821
1822
1823
1824
1825
1826
1827
1828
1829
1830
1831
1832
1833
1834
1835

1836 R scDRS ANALYSIS
1837

1838 **Optimization setup.** scDRS’ codebase consists of several files. We construct a version of
1839 compute_score.py that exposes the compute_raw_score function. This is the only function TusoAI op-
1840 erates upon during optimization. For optimization, we construct causal simulations similar to the
1841 scDRS paper, subsampling 10k cells from TMS, perturbing 1000 disease genes in a cluster of cells,
1842 setting the geneset overlap to 25%, and varying effect size from 5 to 50%. TusoAI optimizes the
1843 compute_raw_score function based on the average ($F1 + AUPRC)/2$ across 3 replicates at effect size
1844 15%, where scDRS has lower power. We run this experiment for 24 hours using default parameter
1845 settings for TusoAI.

1846 **Additional simulation results.** We apply scDRS and the learned version by TusoAI to all 30 repli-
1847 cates of each effect size in causal simulations. We additionally apply it to 100 replicates of null
1848 simulations, identical to scDRS, where 1000 random genes are selected with no perturbation. Addi-
1849 tional metrics in these simulations are reported in Figure 15.



1863 **Figure 15: Additional scDRS metrics.** (A) Q-Q plot of $-\log_{10} p$ -values in null simulations. 95%
1864 CI’s are calculated at each point across 30 replicates. (B) AUPRC of associating individual cells
1865 in causal simulations. 95% CI’s are calculated at each point across 30 replicates. (C) FDR of
1866 associating individual cells in causal simulations. 95% CI’s are calculated at each point across 30
1867 replicates.

1868
1869
1870
1871
1872
1873
1874
1875
1876
1877
1878
1879
1880
1881
1882
1883
1884
1885
1886
1887
1888
1889

1890 S PGBOOST ANALYSIS
1891

1892 **Optimization setup.** pgBoost discovers that distance-based features are critical for modeling SNP-
1893 gene distances. Its samples are SNP-gene pairs, and features include over 30 features derived from
1894 single-cell multiome methods and 2 distance features, the SNP distance to the gene’s transcrip-
1895 tion start site (TSS), and a binary indicator of if this is the closest TSS of any gene to the SNP.
1896 We augment pgBoost’s script with gene annotations from GENCODE V48 (Mudge et al., 2025),
1897 specifically the SNP’s position, the gene’s TSS, and the gene’s transcription end site (TES). During
1898 both the knowledge tree construction and optimization process, TusoAI is encouraged to come up
1899 with instructions/optimizations relevant to distance-based modeling of SNP-gene links and avoid
1900 other model changes. Optimization is performed by increasing the average enrichment in pgBoost’s
1901 primary evaluation of gold-standard links (eQTL and ABC) relative to the original pgBoost’s en-
richment. We run TusoAI for 24 hours using default parameter settings.

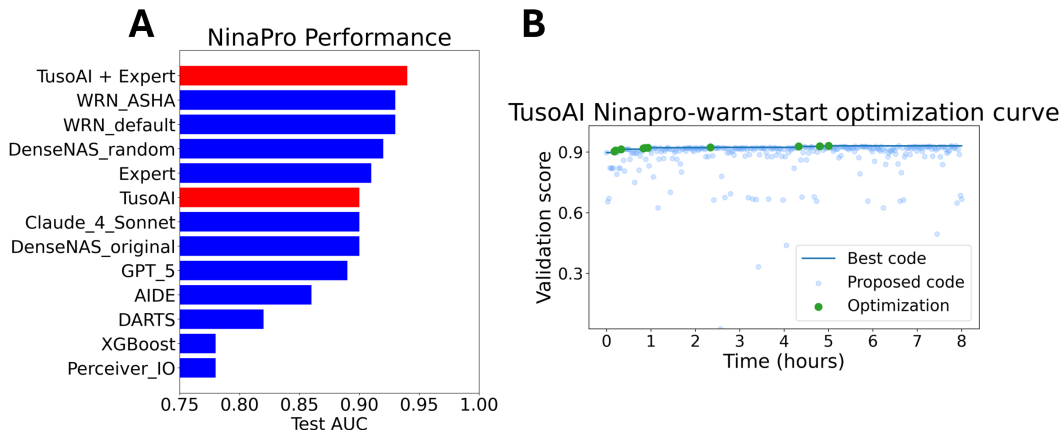
1902 **Real data analysis.** We analyze fine-mapped SNPs from the same set of GWAS traits as in the
1903 pgBoost paper. pgBoost considers a true link to be in the top 95% percentile, and specifically looks
1904 for SNP-gene links that are not in such a percentile for other methods. We perform an identical
1905 analysis, looking for links in the top 95% of pgBoost (TusoAI), but not in other methods.
1906

1907
1908
1909
1910
1911
1912
1913
1914
1915
1916
1917
1918
1919
1920
1921
1922
1923
1924
1925
1926
1927
1928
1929
1930
1931
1932
1933
1934
1935
1936
1937
1938
1939
1940
1941
1942
1943

1944 T WARM START DEEP LEARNING

1945
 1946 We show how TusoAI’s warm-start capability might work in conjunction with a scientific deep
 1947 learning task. For NinaPro, we re-implement the Expert model from NASBench-360. This is a
 1948 feed-forward neural network with attention modules in place of optimizations. Optimizing this
 1949 model for 8 hours with TusoAI improves testing performance from 0.91 to 0.94, now becoming
 1950 the top performing model for this task (Figure 16). Where both the Expert and cold-start TusoAI’s
 1951 learned models were outperformed by NAS methods, their combination yields a new top model. We
 1952 next analyze the optimization trajectory of TusoAI to see how this was achieved. We summarize the
 1953 key optimizations below:

- 1954 1. The dense attention network was replaced with a dilated temporal convolutional network
 1955 (TCN).
- 1956 2. Five separate TCN models were trained and ensembled.
- 1957 3. Features were standardized with z-scaling.
- 1958 4. Gradient clipping.
- 1959 5. Log transformation of input features.
- 1960 6. Ensemble is replaced by a mixture of experts (MOE) architecture.



1979 Figure 16: **Warm start example on NinaPro.** (A) Testing performance of all NinaPro methods.
 1980 (B) Optimization trajectory of TusoAI with warm-start NinaPro.

1998 U PROMPT TEMPLATES

1999

2000 U.1 INSTRUCTIONS FOR PARSING LITERATURE

2001

2002 **Initializing paper description with abstract**

2003

2004 You are a scientific summariser. Draft a concise yet technically accurate description of the
2005 paper's method based **only** on the abstract below, to the extent possible. Capture the
2006 main points using bullet points. Avoid complete sentences and omit details irrelevant to the
2007 methods.

2008 Abstract: " "[ABSTRACT GOES HERE]" "

2009

2010 **Updating paper description with methods section**

2011

2012 The current method description:

2013 " "[CURRENT DESCRIPTION GOES HERE]" "

2014 New excerpt from the paper:

2015 " "[NEW TEXT GOES HERE]" "

2016 Update the description by **incorporating any new technical details or correcting existing**
2017 **ones** found in the excerpt. Keep the description concise and clear. Return **only**
2018 the revised description. Use bullet points. Avoid full sentences and exclude information
2019 unrelated to the methods. Do not exceed 15 bullet points.

2020

2021

2022

2023

2024

2025

2026

2027

2028

2029

2030

2031

2032

2033

2034

2035

2036

2037

2038

2039

2040

2041

2042

2043

2044

2045

2046

2047

2048

2049

2050

2051

2052
2053

U.2 INSTRUCTIONS FOR CONSTRUCTING CATEGORIES

2054
2055**Initializing categories with LLM**

2056

We are building an LLM-powered AutoML system for the task:
"[TASK DESCRIPTION]"

2057

As a reference, some generic categories for optimizing classification models include:
[CLASSIFICATION CATEGORIES]

2058

You are a master of machine learning and the domain relevant to this task. First briefly reason
about what kinds of modeling interventions or optimization strategies could be helpful for
this specific task. Then propose a list of concise, task-relevant optimization categories.

2059

Your list should include conceptual ideas tailored to this task and each should represent a
specific axis of improvement (e.g., architectural choices, preprocessing strategies, domain
constraints, evaluation metrics, robustness techniques, etc.).

2060

Output exactly **N** proposed categories, one per line, each enclosed in:

2061

<c>Category Name</c>

2062

Do not include any other text, explanation, or formatting. By "optimization" we mean
strictly performance improvements — not runtime, scalability, visualization, logging, post-
evaluation tools, or similar considerations. You will only have access to: [DATA AVAIL-
ABLE].

2063

2064

Updating categories with papers

2065

We are building an LLM-powered AutoML system for the task:
"[TASK DESCRIPTION]"

2066

We will curate and refine our categories based on the current categories and a paper.

2067

Current categories: [CURRENT CATEGORIES]

2068

Paper: "[TITLE]" Key method points: [BULLET POINTS]

2069

TASK 1. If the paper suggests a **new** axis of optimization missing from the list, propose
a concise, task-relevant category for it. 2. If two or more current categories can be merged,
provide a single category name that subsumes them. 3. Otherwise, if a category is irrelevant
given only [DATA AVAILABLE], leave the list unchanged.

2070

Return **one updated list only**, one category per line. Each line must be wrapped exactly
like:

2071

<c>Category</c>

2072

No other text.

2073

2074

2075

2076

2077

2078

2079

2080

2081

2082

2083

2084

2085

2086

2087

2088

2089

2090

2091

2092

2093

2094

2095

2096

2097

2098

2099

2100

2101

2102

2103

2104

2105

2106 U.3 INSTRUCTIONS FOR CONSTRUCTING WITHIN-CATEGORY INSTRUCTIONS
21072108 **Initializing within-category instructions with LLM**
21092110 We are designing an LLM-powered AutoML system for the task:
2111 "[TASK DESCRIPTION]"2112 Current optimisation axis: **[CATEGORY]**
2113 Below is a style example of prompts for a *regularisation* category for a classification task.
2114 Each prompt begins with *by ...* and expresses a specific, actionable optimisation idea:
2115 [FEW-SHOT EXAMPLES]2116 You are a master of machine learning and the domain relevant to this task. Keeping the same
2117 concise, actionable style, write **exactly N distinct prompts** that belong to the **[CATE-
2118 GORY]** category **and are appropriate for this task**.2119 These should include a mix of general, conceptual, and complex prompts, not overly spe-
2120 cific, similar to the examples.

2121 Wrap *each* prompt in its own:

2122 <p> ... </p>
2123 Return **only** these <p>...</p> lines, nothing else.2124 By optimisation we mean strictly **performance**, not runtime, scalability, logging, visu-
2125 alization, evaluation, or post-processing. Assume evaluation metrics already exist. You will
2126 only have access to: [DATA AVAILABLE].2127 **Refining within-category instructions with LLM**
21282129 We are designing an LLM-powered AutoML system for the task:
2130 "[TASK DESCRIPTION]"

2131 We will only have access to: [DATA AVAILABLE].

2132 Here is a concise summary of the baseline method: """"[SUMMARY]""""

2133 Below are style examples of valid prompt lines taken from earlier work: [FEW-SHOT EX-
2134 AMPLES]2135 Your job is to generate **between N_min and N_max new prompts**. These prompts will
2136 ultimately be assigned to one of the following categories:

2137 [CATEGORY LIST]

2138 **Step 1**: Generate the prompts, independently of categories. **Step 2**: Assign each
2139 prompt to its most relevant category.

2140 For each prompt, output a line in this exact format:

2141 <c>CategoryName</c><p>by ...</p>

2142 Rules:

2143 * Every prompt must begin with **"by ..."** * Cover a mix of general, conceptual, and
2144 complex ideas * Focus strictly on **performance optimisation** (ignore runtime, scalabil-
2145 ity, logging, visualization, etc.) * Return **only** the <c>...</c><p>...</p> lines —
2146 nothing else.

2147

2148

2149

2150

2151

2152

2153

2154

2155

2156

2157

2158

2159

2160
2161

U.4 INSTRUCTIONS FOR CONSTRUCTING INITIAL SOLUTIONS

2162
2163**Initializing solutions with LLM**2164
2165

We are designing an LLM-powered AutoML system for the task:
"[TASK DESCRIPTION]"

2166
2167

Below is an example list of generic model initializations for a **classification** task: [FEW-SHOT EXAMPLES]

2168
2169

You are a master of machine learning and of the domain relevant to this task. Propose **exactly N concise model initializations** that could serve as starting baselines **for this specific task**, given that we only have [DATA AVAILABLE].

2170
2171

These should be general task-specific methods, model families, or high-level architectural descriptions — not fully specified pipelines.

2172
2173

Output one per line, each wrapped in:

<m> ... </m>

2174
2175

Return **only** these <m>...</m> lines — no explanations, no extra text.

2176
2177**Refining initial solutions with LLM**

2178

We are building an LLM-powered AutoML system for the task:
"[TASK DESCRIPTION]"

2180
2181

We will curate and refine our **model initializations** list using insights from the following paper.

2182

Current initializations: [CURRENT INITIALIZATIONS]

2183

Paper: "[TITLE]" Key method points: [BULLET POINTS]

2184
2185

TASK → 1. If the paper presents a **model family or architecture** not covered above, propose it as a concise initialization (≤ 6 words). 2. If two or more current initializations are effectively the same family, merge them by giving a single, clear name that subsumes them. 3. If neither condition applies, or if the model cannot be implemented using **[DATA AVAILABLE]**, leave the list unchanged.

2188
2189

Return **one updated list only** — one initialization per line, each wrapped exactly like:

<m>Initialization</m>

2190
2191

No other text.

2192
21932194
21952196
21972198
21992200
22012202
22032204
22052206
22072208
22092210
22112212
2213

2214 **U.5 PROMPT FOR DEVELOPING INITIAL SOLUTIONS**
2215

2216 **Initialisation prompt**

2218 Write a basic version of this model for {task_description} using {init}. Hints: - {hints}
2219 {base_fn_code} Output only python code, and do not include comments.
2220

2221

2222

2223

2224

2225

2226

2227

2228

2229

2230

2231

2232

2233

2234

2235

2236

2237

2238

2239

2240

2241

2242

2243

2244

2245

2246

2247

2248

2249

2250

2251

2252

2253

2254

2255

2256

2257

2258

2259

2260

2261

2262

2263

2264

2265

2266

2267

2268 U.6 PROMPT FOR OPTIMIZING WITH INSTRUCTIONS
2269

2270 **Instruction-based optimization prompt**
2271

2272 Write a basic version of this model for {task_description} using {init}. Hints: - {hints}
2273 {base_fn_code} Output only python code, and do not include comments.
2274 by choosing one of the following strategies to guide optimisation, based on your assessment
2275 of what will most improve this model for {task_description}: {prompt_options}
2276 Additionally, consider the following feedback from earlier attempts that used this same op-
2277 timisation strategy: {fb_block}

2278
2279
2280
2281
2282
2283
2284
2285
2286
2287
2288
2289
2290
2291
2292
2293
2294
2295
2296
2297
2298
2299
2300
2301
2302
2303
2304
2305
2306
2307
2308
2309
2310
2311
2312
2313
2314
2315
2316
2317
2318
2319
2320
2321

2322 U.7 PROMPT FOR GENERATING DIAGNOSTICS
2323

2324 **Generating diagnostic info prompt**
2325

2326 Write a basic version of this model for {task_description} using {init}. Hints: - {hints}
2327 {base_fn_code} Output only python code, and do not include comments.
2328 by choosing one of the following strategies to print diagnostic information, based on
2329 your assessment of what will be most informative for optimisation of this model for
2330 {task_description}. Ensure the information printed is concise enough to be used in an LLM
2331 prompt: {diagnostic_options}

2332
2333 U.8 PROMPT FOR OPTIMIZING WITH DIAGNOSTICS
2334

2335 **Optimizing with diagnostic info prompt**
2336

2337 Write a basic version of this model for {task_description} using {init}. Hints: - {hints}
2338 {base_fn_code} Output only python code, and do not include comments.
2339 by assessing this diagnostic info and proposing model/feature improvements for this model
2340 for {task_description}: {current_code}
2341 Additionally, consider the following feedback from earlier attempts that used this same op-
2342 timisation strategy: {fb_block}

2343
2344
2345
2346
2347
2348
2349
2350
2351
2352
2353
2354
2355
2356
2357
2358
2359
2360
2361
2362
2363
2364
2365
2366
2367
2368
2369
2370
2371
2372
2373
2374
2375

2376 U.9 PROMPT FOR GENERATING FEEDBACK
2377

2378 **Feedback on code optimization**
2379

2380 We attempted to optimize this function: [ORIGINAL_CODE] Here is the proposed opti-
2381 mization: [NEW_CODE] Write a concise one line summary of the differences between the
2382 original function and the proposed optimization. It should be as short as possible while
2383 summarizing the differences.

2384
2385
2386
2387
2388
2389
2390
2391
2392
2393
2394
2395
2396
2397
2398
2399
2400
2401
2402
2403
2404
2405
2406
2407
2408
2409
2410
2411
2412
2413
2414
2415
2416
2417
2418
2419
2420
2421
2422
2423
2424
2425
2426
2427
2428
2429

2430 U.10 PROMPT FOR DEBUGGING
2431

2432 **Fix Function Prompt**

2433
2434 Fix this function: {suggestion}. Here's the error: {error_msg} Ignore warnings. If an error
2435 is related to installation, assume the package is not installed and try doing it without that
2436 specific package. Output only python code, and do not include comments.
2437

2438

2439

2440

2441

2442

2443

2444

2445

2446

2447

2448

2449

2450

2451

2452

2453

2454

2455

2456

2457

2458

2459

2460

2461

2462

2463

2464

2465

2466

2467

2468

2469

2470

2471

2472

2473

2474

2475

2476

2477

2478

2479

2480

2481

2482

2483

2484 U.11 PROMPT TEMPLATE FOR BIOMNI AND CHATGPT-AGENT
 2485

2486 2487 **Single-cell denoising prompt template for scientific agents**

2488
 2489 We are considering the task of single cell RNA-seq imputation.
 2490 We wish to create an expertly optimized model **for** this.
 2491 Here **is** a starter script. Create a top-performing model **for** our task within the
 tuso_model function.
 2492
 2493 import scanpy as sc
 2494 import pandas as pd
 2495 import numpy as np
 2496 import scipy as sp
 2497 import magic
 2498 from anndata import read_h5ad
 2499 import scprep
 2500 from scipy.sparse import csr_matrix
 2501 from sklearn.neighbors import NearestNeighbors
 2502 from scipy.sparse import issparse
 2503 from sklearn.decomposition import PCA
 2504 from anndata import AnnData
 2505 import random
 2506
 2507 def mse(adata):
 2508 import anndata
 2509 import scanpy as sc
 2510 import scprep
 2511 import sklearn.metrics
 2512
 2513 test_data = anndata.AnnData(X=adata.obsm["test"], obs=adata.obs, var=adata.var)
 2514 denoised_data = anndata.AnnData(
 2515 X=adata.obsm["denoised"], obs=adata.obs, var=adata.var
 2516)
 2517
 2518 # scaling and transformation
 2519 target_sum = 10000
 2520
 2521 sc.pp.normalize_total(test_data, target_sum=target_sum)
 2522 sc.pp.log1p(test_data)
 2523
 2524 sc.pp.normalize_total(denoised_data, target_sum=target_sum)
 2525 sc.pp.log1p(denoised_data)
 2526
 2527 error = sklearn.metrics.mean_squared_error(
 2528 scprep.utils.toarray(test_data.X), denoised_data.X
 2529)
 2530 return error
 2531 def tuso_model(adata):
 2532 a = AnnData(
 2533 X=adata.obsm["train"].copy(),
 2534 obs=adata.obs.copy(),
 2535 var=adata.var.copy()
 2536)
 2537
 2538 out = a.X
 2539 out = out.toarray() **if** issparse(out) **else** out
 2540 adata.obsm["denoised"] = out
 2541 return adata
 2542 def main():
 2543 np.random.seed(42)
 2544 random.seed(42)
 2545 adata = read_h5ad('1k_pbmc_processed.h5ad')
 2546 **print**("tuso_model_start")
 2547 adata = tuso_model(adata)
 2548 **print**("tuso_model_end")
 2549
 2550 val_metric = 1-mse(adata)
 2551 **print**(f"tuso_evaluate: {val_metric}")
 2552
 2553 main()
 2554
 2555
 2556 Make sure to store the denoised data **in** adata.obsm["denoised"].
 2557 Keep the function header, **input**, output the same.
 2558

2538

2539

2540

Each time you generate code, run it, extract the tuso_evaluate metric, **and try and**
build a better performing solution **from** the previous solutions.

2541

2542

2543

2544

2545

2546

2547

2548

2549

2550

2551

2552

2553

2554

2555

2556

2557

2558

2559

2560

2561

2562

2563

2564

2565

2566

2567

2568

2569

2570

2571

2572

2573

2574

2575

2576

2577

2578

2579

2580

2581

2582

2583

2584

2585

2586

2587

2588

2589

2590

2591

2592 **V GENERIC CLASSIFICATION EXAMPLE**
2593

2594 List	2595 Contents
2596 Categories	['regularisation', 'feature_engineering', 'hyperparameter_tuning', 'sampling', 'ensemble_methods', 'calibration', 'feature_selection']
2597 Initializations	["logistic regression", "XGBoost", "random forest", "MLP classifier"]
2598 Regularisation 2599 instructions	<ol style="list-style-type: none"> 1. by introducing L1 sparsity constraints to prune features 2. by subsampling training rows each iteration to inject stochasticity 3. by shrinking updates with a smaller learning rate for smoother convergence 4. by refining regularisation strategies 5. by combining complementary regularisation methods 6. by adapting regularisation strength across epochs 7. by scaling regularisation to the dataset size 8. by combining elastic-net with adaptive polynomial penalties to capture curved relationships 9. by adding Jacobian norm regularisation to control sharp non-linear gradients 10. by introducing spectral norm constraints for stable non-linear layers

2600
2601
2602
2603
2604
2605
2606
2607
2608
2609
2610
2611
2612
2613
2614
2615
2616
2617
2618
2619
2620
2621
2622
2623
2624
2625
2626
2627
2628
2629
2630
2631
2632
2633
2634
2635
2636
2637
2638
2639
2640
2641
2642
2643
2644
2645